Molecular Therapy
Original Article

# *Otx2*-Genetically Modified Retinal Pigment Epithelial Cells Rescue Photoreceptors after Transplantation

Christo Kole,[1,2,3] Laurence Klipfel,[1,2,3] Ying Yang,[1,2,3,5] Vanessa Ferracane,[1,2,3,5] Frederic Blond,[1,2,3] Sacha Reichman,[1,2,3] Géraldine Millet-Puel,[1,2,3] Emmanuelle Clérin,[1,2,3] Najate Aït-Ali,[1,2,3] Delphine Pagan,[1,2,3] Hawa Camara,[1,2,3] Marie-Noëlle Delyfer,[1,2,3,4] Emeline F. Nandrot,[1,2,3] Jose-Alain Sahel,[1,2,3] Olivier Goureau,[1,2,3] and Thierry Léveillard[1,2,3]

[1]INSERM, U968, Paris 75012, France; [2]Sorbonne Universités, UPMC Univ Paris 06 UMR_S 968, Institut de la Vision, Paris 75012, France; [3]CNRS, UMR_7210, Paris 75012, France; [4]Unité Rétine, Uvéite et Neuro-Ophtalmologie, Département d'Ophtalmologie, Centre Hospitalier Universitaire de Bordeaux, Bordeaux, France

**Inherited retinal degenerations are blinding diseases characterized by the loss of photoreceptors. Their extreme genetic heterogeneity complicates treatment by gene therapy. This has motivated broader strategies for transplantation of healthy retinal pigmented epithelium to protect photoreceptors independently of the gene causing the disease. The limited clinical benefit for visual function reported up to now is mainly due to dedifferentiation of the transplanted cells that undergo an epithelial-mesenchymal transition. We have studied this mechanism in vitro and revealed the role of the homeogene OTX2 in preventing dedifferentiation through the regulation of target genes. We have overexpressed OTX2 in retinal pigmented epithelial cells before their transplantation in the eye of a model of retinitis pigmentosa carrying a mutation in *Mertk*, a gene specifically expressed by retinal pigmented epithelial cells. OTX2 increases significantly the protection of photoreceptors as seen by histological and functional analyses. We observed that the beneficial effect of OTX2 is non-cell autonomous, and it is at least partly mediated by unidentified trophic factors. Transplantation of OTX2-genetically modified cells may be medically effective for other retinal diseases involving the retinal pigmented epithelium as age-related macular degeneration.**

## INTRODUCTION

Retinitis pigmentosa is the most prevalent form of inhered retinal degeneration, which is characterized clinically by two successive phases. Nyctalopia, or night blindness, which constitutes the first symptom, corresponds to a moderate handicap for the patients compared to the second phase of reduction of the visual field that often leads to blindness. These two phases result from two waves of photoreceptor degeneration: the rods that are responsible of vision at low luminance and the cones on which vision relies during daytime. Inherited retinal diseases are characterized genetically by their extreme heterogeneity, with a significant proportion of genes causing retinitis pigmentosa expressed specifically by rods.[1] Mutations in genes expressed by the retinal pigment epithelium (RPE) have also been reported to cause retinitis pigmentosa.[2] The RPE has a pivotal role in the function of photoreceptor cells. Any abnormality that affects this tissue or its degeneration has a direct impact in vision, often leading to blindness.[3–5]

Depending on the primary genetic defect, different strategies have been applied to limit the progress of photoreceptor degeneration. A severe form of recessive inherited retinal degeneration, Leber congenital amaurosis, was successfully treated by corrective gene therapy in the case of mutations in the *RPE65* gene.[6] Nevertheless, the impact on the disease is limited to those patients; therefore, alternative approaches that are independent of the causative genes have been studied. Because of the essential role of cones for vision, we have concentrated our efforts on the prevention of secondary cone loss in retinitis pigmentosa. The identification of rod-derived cone viability factor (RdCVF) initiates therapeutic development based on the administration of this novel trophic factor, normally secreted by rods, to prevent cone degeneration and vision loss in retinitis pigmentosa patients.[7,8] The treatment would be almost independent of the causative gene for both recessive and dominant forms of retinitis pigmentosa.[8,9]

Nevertheless, when the RPE is damaged, like in Best's disease, transplantation of healthy RPE cells will be necessary.[10,11] Regardless of photoreceptor rescue in animal models,[10,12] visual recovery after RPE transplantation in human trials is scarce, and full visual recovery has not been demonstrated.[11,13–15] This limited success might be due to the dedifferentiation of RPE cells. When cultured, a necessary process to enrich the material to be grafted, RPE cells dedifferentiate into mesenchymal cells.[16] Even grafted RPE cells dedifferentiate into

Received 30 January 2015; accepted 3 September 2017;
https://doi.org/10.1016/j.ymthe.2017.09.007.

[5]These authors contributed equally to this work.

**Correspondence:** Thierry Léveillard, Institut de la Vision, Université Pierre et Marie Curie, Paris 75012, France.
**E-mail:** thierry.leveillard@inserm.fr

spindle-shaped cells resembling fibroblasts and macrophages in the subretinal space.[14] This transformation is undesirable, because it is a risk factor for its complication, proliferative vitreoretinopathy.[17] The mechanisms regulating RPE dedifferentiation are presently unknown. Here, by studying RPE dedifferentiation in vitro, we revealed downregulation of orthodenticle homolog of *Drosophila* (OTX2), a gene essential for the development and the maintenance of the RPE.[18,19] Therefore, we thought that OTX2 might be able to counteract RPE cell dedifferentiation. We also demonstrated the benefit of transplanting genetically modified RPE cells overexpressing OTX2 on photoreceptor function and survival in a retinitis pigmentosa model with a mutation in a gene specifically expressed by the RPE. Our data provide the rational for improving treatments of inherited retinal diseases.

## RESULTS

### Cultured Retinal Pigment Epithelial Cells Undergo a Transient Epithelial-Mesenchymal Transition

We found that culturing primary pig RPE cells for one week induces the expression of two mesenchymal markers, alpha smooth-muscle actin (*ACTA2*) and vimentin (*VIM*) (Figure 1A). Similar epithelial-mesenchymal transition has been reported for RPE cells in vitro.[20] The cells expressing ACTA2 have distinctive morphology and are absent in confluent cell cultures at three weeks (Figure 1B). To elucidate the mechanism underlying this transient transition, we measured the expression of a subset of 37 genes selected for being specifically expressed by RPE cells, presumably implicated in RPE function or photoreceptor survival.[21–25] We found that 27 of these genes (73%) were downregulated in primary cultured RPE cells, while three genes were upregulated: *SLC16A3*, *SLC16A12*, and *TYRP1* (Figure 1C; Table 1). Among the downregulated genes, we noticed the presence of two transcription factors, CRX and OTX2. The expression of *CRX* was severely reduced, while that of *OTX2* was halved. We subsequently focused on transcription factors due to their ability to regulate gene networks and for their potential importance in the observed dedifferentiation process. Because it has been reported that OTX2 regulates the expression of *CRX* and that consequently *CRX* is downstream of *OTX2*, we examined OTX2 expression by western blot.[26] We confirmed that OTX2 protein expression is reduced after one week in culture (Figure 1D). The signal that corresponds to the OTX2 splice variant OTX2L seems to be induced during the epithelial-mesenchymal transition process. OTX2L encoded for an additional octapeptide GPWASCPA, 5 amino acids upstream of the homeodomain, but no additional function has been attributed to this variant.[27]

An epithelial-mesenchymal transition has also been reported to occur in vivo, following retinal detachment and leading to proliferative vitreoretinopathy.[17] We examined the expression of *VIM* in 19 human surgical specimens of retinal detachment compared to 19 post-mortem specimens of neural retina by qRT-PCR. A 2.37-fold elevation of *VIM* expression correlates with retinal detachment (Figure 1E). In the same specimens, *OTX2* expression is reduced by 2.17-fold. The inwardly rectifying potassium channel KIR7.1, encoded by the *KCNJ13* gene, is also downregulated. Nevertheless, this correlation is not sufficient to conclude that downregulation of OTX2 is triggering the epithelial-mesenchymal transition. Mutations in *KCNJ13* cause Leber congenital amaurosis, a blinding disease, and snowflake vitreoretinal degeneration, an autosomal dominant retinal disease, leading to retinal detachment, among other deficits.[28–30]

### Identification of Novel OTX2 Target Genes in RPE

To test whether OTX2 regulates the expression of the 27 downregulated genes, we overexpressed rat OTX2, as well as independently overexpressed OTX2L in pig primary RPE cells. OTX2 and OTX2L cDNAs were cloned into an adeno-associated virus (AAV) vector, adeno-associated virus 2 serotype 1 (AAV2.1), and RPE cells were infected by AAV2.1-GFP, AAV2.1-OTX2, or AAV2.1-OTX2L. Seven days after transduction, the expression of OTX2 was verified by qRT-PCR using primers that do not discriminate pig from rat *OTX2* mRNA (Figure 2A). The nucleotide sequence of rat and pig OTX2 are 93% identical over the coding sequences, so specific primers could not be designed. The same set of primers was used for both OTX2 and OTX2L, permitting direct comparison. We noticed that ectopic expression of OTX2 reduces the expression of *VIM* by 4-fold (Figure 2B). Western blot analysis allowed us to evaluate the level of OTX2 overexpression in that system, because the antibodies used do not distinguish the ectopic rat from endogenous pig OTX2 (Figure 2C). This analysis shows that the expression of VIM protein is reduced by ectopic OTX2. Considering that the splicing variant OTX2L does not differ from OTX2 in its transcriptional properties when tested, we did not test for the effect of OTX2L on VIM expression. When we examined the expression of ACTA2, the second maker of epithelial-mesenchymal transition, we did not observe a reduction in the number of epithelial-mesenchymal transition-like cells (Figure 2D). This suggested to us that OTX2 might have other unidentified targets. Among the 37 selected genes, we found that *CRX* expression is increased by almost 20-fold by both OTX2 and OTX2L, confirming that OTX2 controls the expression of *CRX* in RPE cells (Figure 2E). Similarly, the tyrosinase gene *TYR* is increased by 15-fold, most likely through binding of OTX2 to the *TYR* promoter, as reported.[18] The tyrosinase-related protein gene *DCT* and *KCNJ13* are increased by OTX2 (~9-fold) and OTX2L (5- to 6-fold). Finally, the keratin gene *KRT18*, the retinol dehydrogenase gene *RDH10*, *TYPR1*, and the monocarboxylic acid transporter genes *SLC16A8* and *SLC16A12* are increased by 2- to 5-fold (Table 2). The observed upregulation of *SLC16A12* concomitantly to OTX2 downregulation in Figure 1C and its increase in expression in the presence of OTX2 in Figure 2E suggest that during dedifferentiation, an unidentified transcription factor activity that targets the *SLC16A12* promoter is increased, exerting a dominant effect over that of OTX2 on the same promoter in different experimental conditions. To further establish the role of OTX2 in regulating the expression of these genes at the transcriptional level, we performed chromosomal immunoprecipitation on uninfected primary pig RPE cells. *TYRP1* was used as a positive control, because OTX2 has been reported to bind OTX2 regulatory elements within this promoter.[18]

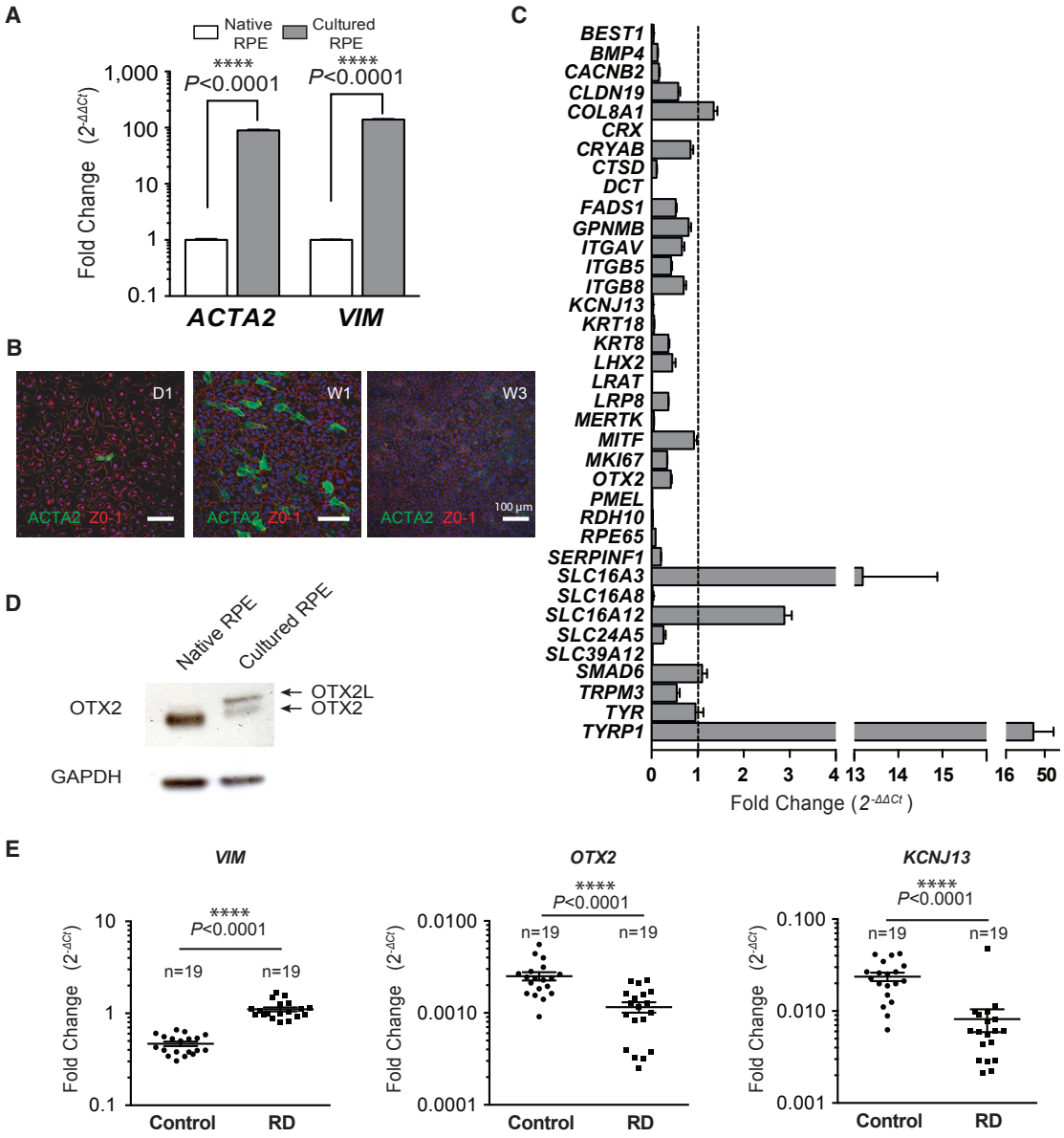


**Figure 1. Cultured Retinal Pigment Epithelial Cells Undergo a Transient Epithelial-Mesenchymal Transition**

(A) Overexpression of mesenchymal markers, alpha smooth-muscle actin (*ACTA2*) and vimentin (*VIM*) in cultured RPE cells measured by qRT-PCR. (B) Immunocytological analysis of pig primary RPE culture at 1 and 3 weeks using anti-ACTA2 and anti-ZO-1 antibodies. (C) Relative qRT-PCR analysis of genes performed on cultured and native RPE cells. All samples were normalized to *GAPDH*. Mean with SD (n = 3, multiple comparison test). (D) Western blot analysis of OTX2 expression in native and cultured RPE cells. (E) Relative qRT-PCR analysis of *OTX2*, *KCNJ13*, and *VIM* in patients after retinal detachment (RD) and post-mortem normal specimens normalized to *GAPDH*. Individual data are shown as points. Mean with SEM (n = 19, t test, Welch correction).

Candidate OTX2 regulatory elements were found in the *KCNJ13*, *RDH10*, and *SLC16A12* promoters (Figure 2F). Anti-OTX2 co-immunoprecipitated TYRP1 promoter DNA, while no signal was observed when immunoglobulins, such as immunoglobulin G (IgG), were omitted (−IgG) and only a weak signal was observed when using immunoglobulins that are non-specific for OTX2 (+IgG), demonstrating that OTX2 binds specifically to the *TYRP1* promoter (Figure 2G). Similar results were obtained with two genes, *KCNJ13* and *RDH10*, whose expression is induced by OTX2. A third one, *SLC16A12*, shows some degree of co-immunoprecipitation, although the result is less clear for reasons linked to the PCR primers used. The *β-globin* (*HGB*) promoter was used as negative control. An unambiguous demonstration could be achieved using qPCR.

**Table 1. Relative Expression in Cultured RPE versus Native RPE Cells**

| Gene Symbol | Gene Name | NCBI Accession No. | Relative Expression ($2^{-\Delta\Delta Ct}$) | p Value |
|---|---|---|---|---|
| Downregulated Genes | | | | |
| *BEST1* | bestrophin 1 | XM_003353833.1 | 0.043 | <0.0001 |
| *BMP4* | bone morphogenetic protein 4 | NM_001101031.2 | 0.132 | <0.0001 |
| *CACNB2* | calcium channel voltage dependent beta 2 | XM_003482816.1 | 0.161 | <0.0001 |
| *CLDN19* | claudin-19 | NM_001160084.1 | 0.580 | 0.0006 |
| *CRX* | cone-road homeobox | XM_003127265.1 | 0.001 | <0.0001 |
| *CTSD* | cathepsin D | NM_001037721.1 | 0.108 | <0.0001 |
| *DCT* | dopachrome tautomerase | NM_001025227.1 | 0.001 | <0.0001 |
| *FADS1* | fatty acid desaturase 1 | NM_001113041.1 | 0.526 | 0.0002 |
| *ITGB5* | integrin, beta 5 | NM_001246669.1 | 0.427 | <0.0001 |
| *KCNJ13* | potassium inwardly rectifying channel subfamily J,13 | XM_001926506.3 | 0.033 | <0.0001 |
| *KRT8* | keratin 8 | NM_001159615.1 | 0.364 | <0.0001 |
| *KRT18* | keratin 18 | XM_003126180.3 | 0.058 | <0.0001 |
| *LHX2* | lim homeobox protein 2 | NM_001170519.1 | 0.452 | 0.0004 |
| *LRAT* | lecithin-retinol acyltransferase | NM_001244920.1 | 0.014 | <0.0001 |
| *LRP8* | apolipoprotein e receptor | NM_001199891.1 | 0.365 | <0.0001 |
| *MERTK* | c-mer proto-oncogene tyrosine kinase | XM_003124812.3 | 0.052 | <0.0001 |
| *MKI67* | marker of proliferation ki-67 | NM_001101827.1 | 0.338 | <0.0001 |
| *OTX2* | orthodenticle homolog 2 | XM_003353491.1 | 0.422 | <0.0001 |
| *PMEL* | premelanosome protein | XM_003481626.1 | 0.018 | <0.0001 |
| *RDH10* | retinol dehydrogenase 10 | XM_001928082.3 | 0.031 | <0.0001 |
| *RPE65* | retinal pigment epithelium 65 kDa | XM_003127931.2 | 0.088 | <0.0001 |
| *SERPINF1* | serpin peptidase inhibitor | NM_001078662.1 | 0.207 | <0.0001 |
| *SLC16A8* | solute carrier family 16, member 8 | XM_003126028.1 | 0.023 | <0.0001 |
| *SLC24A5* | solute carrier family 24, member 5 | XM_003121523.1 | 0.261 | <0.0001 |
| *SLC39A12* | solute carrier family 39, member 12 | XM_003130728.1 | 0.023 | <0.0001 |
| *TRPM3* | transient receptor potential cation channel | XM_001925032.3 | 0.551 | 0.0008 |
| Upregulated Genes | | | | |
| *SLC16A3* | solute carrier family 16, member 3 | XM_003357925.1 | 13.193 | 0.0002 |
| *SLC16A12* | solute carrier family 16, member 12 | XM_001928811.2 | 2.885 | <0.0001 |
| *TYRP1* | tyrosinase related protein 1 | NM_001025226.1 | 48.561 | <0.0001 |

Relative expression ($2^{-\Delta\Delta Ct}$) of genes in cultured RPE cells normalized by the expression in native RPE cells. Data normalized to *GAPDH*. Statistical analysis: multiple t test and Holm-Sidak method, with alpha = 1.000%, n = 3 biological triplicates.

### OTX2 Induces the Expression of *KCNJ13*, *RDH10*, and *SLC16A8* in Human iPS RPE Cells

To investigate whether these genes are targeted by OTX2 in human RPE cells, we overexpressed OTX2 in RPE derived from human-induced pluripotent stem-derived cells (hiPS-RPE).[31] These hiPS-RPE cells express melanin, have typical cobblestone morphology (Figure 3A), and express the tight junction protein ZO-1 and the transcription factor MITF (Figure 3B). Moreover, the hiPS-RPE cells express RPE markers such as *RPE65*, *MITF*, *BEST1*, *MERTK*, and *RDH10* to levels similar to those expressed by RPE cells isolated from a normal human post-mortem specimen and contrary to the undifferentiated immunoprecipitation (IP) cells, confirming that human-induced pluripotent stem cells (hiPSCs) have differentiated into RPE cells (Figure S1). AAV infection resulted in 8- and 5-fold increases in expression of *Otx2* and *Otx2L*, respectively, over endogenous *OTX2* after seven days, as shown by qRT-PCR (Figure 3C). Using hiPS-RPE, the level of *OTX2L* expression is lower than that of *OTX2*, contrary to what was observed with pig primary RPE cells (Figure 2A). The expression of the tyrosinase gene *TYR* is increased by 30- and 20-fold by OTX2 and OTX2L, respectively, similar to what was observed in the pig RPE cell cultures (Figure 3D). *CRX* expression was increased by 18-fold. Four additional candidate

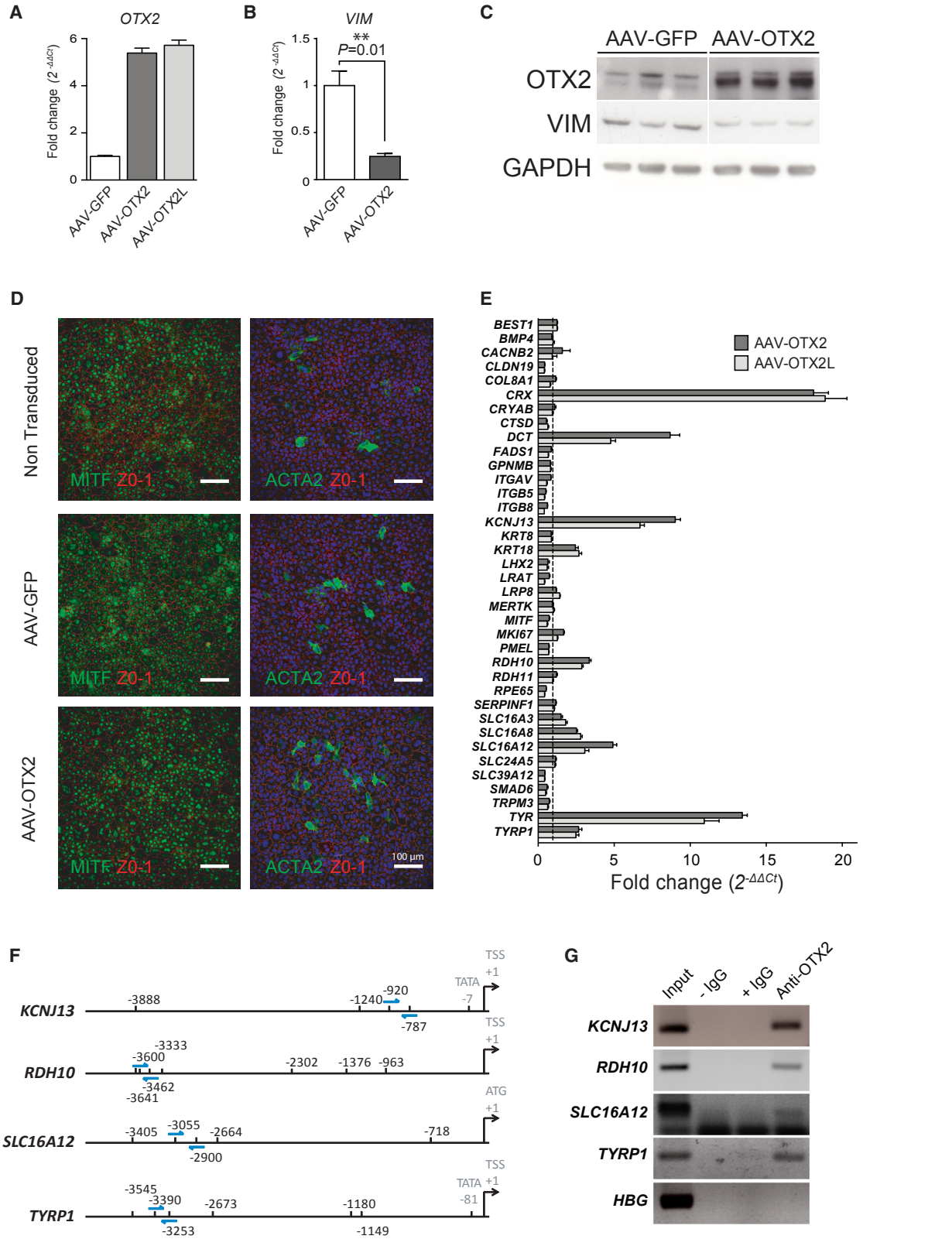


(legend on next page)

**Table 2. Relative Expression in Cultured RPE Transduced with AAV-*Otx2* and AAV-*Otx2L* versus Control Transduced RPE Cells**

| Gene Symbol | Gene Name | Relative Expression ($2^{-\Delta\Delta Ct}$) AAV-OTX2 | AAV-OTX2L | p Value |
|---|---|---|---|---|
| *CACNB2* | calcium channel voltage dependent beta 2 | 1.59 | – | 0.002 |
| *CLDN19* | claudin-19 | 0.42 | 0.41 | 0.003 |
| *CRX* | cone-road homeobox | 18.88 | 18.12 | <0.0001 |
| *DCT* | dopachrome tautomerase | 8.68 | 4.77 | <0.0001 |
| *KCNJ13* | potassium inwardly rectifying channel subfamily J,13 | 9 | 6.77 | <0.0001 |
| *KRT18* | keratin 18 | 2.45 | 2.68 | <0.0001 |
| *MKI67* | marker of proliferation ki-67 | 1.67 | – | 0.0005 |
| *RDH10* | retinol dehydrogenase 10 | 3.36 | 2.87 | <0.0001 |
| *RPE65* | retinal pigment epithelium 65 kDa | – | 0.42 | 0.003 |
| *SLC16A8* | solute carrier family 16, member 8 | 2.52 | 2.79 | <0.0001 |
| *SLC16A12* | solute carrier family 16, member 12 | 4.91 | 3.06 | <0.0001 |
| *SLC39A12* | solute carrier family 39, member 12 | 0.44 | 0.42 | <0.004 |
| *TYR* | tyrosinase | 13.42 | 10.92 | 0.0008 |
| *TYRP1* | tyrosinase related protein 1 | 2.66 | 2.48 | <0.0001 |

Relative expression ($2^{-\Delta\Delta Ct}$) of genes in cultured RPE cells transduced with AAV-*Otx2* and AAV-*Otx2L* normalized by the expression in control cells (AAV-GFP-transduced RPE). Data normalized to *GAPDH*. Statistical analysis: two-way ANOVA and Dunnett test, with alpha = 1.000%, n = 3 biological triplicates.

OTX2-regulated genes were increased by ectopic expression of OTX2 and OTX2L: *KCNJ13* (12.4-fold), *SLC16A12* (3.3-fold), *RDH10* (2.0-fold), and *SLC16A8* (1.8-fold).

### Grafting Genetically Modified RPE Cells Overexpressing OTX2 in RCS Rat Improves Photoreceptor Function

Would the differentiation of RPE cells by OTX2 improve the benefit of transplantation on photoreceptor survival? To answer to this question, we studied the effect of RPE cell transplantation in the royal college of surgeons (RCS) rat, a recessive model of retinitis pigmentosa that carries a recessive mutation in the *rdy* gene encoding for MERTK protein. MERTK is a receptor tyrosine kinase expressed by RPE that is essential to the phagocytosis of the outer segments of photoreceptors.[24] *MERTK* mutations cause retinitis pigmentosa (RP) in human and rod photoreceptors of the RCS to degenerate from post-natal day (P) 23 to P60.[32] The degeneration of rods is soon followed by the degeneration of cones.[10,33] By P60, rod and cone function are not recordable and histological examination shows that the outer nuclear layer (ONL), the layer of photoreceptor cells, is almost lost (Figure 7A).

Using a double-blind procedure, we injected 50,000 RPE cells (n = 7) into the subretinal space of the RCS rat eye at P18, before degeneration starts. GFP-expressing cells cannot be identified before the surgery in this setting. Because it was not possible to prepare enough human iPS-RPE cells for this study, we used pig RPE cells. The injection was made in the dorsal part of the retina of right eyes, while left eyes remained untreated. One week before transplantation, pig RPE cells were infected with a recombinant AAV2.1 vector encoding for GFP or OTX2. AAV2.1-GFP-transduced RPE (RPE-GFP) cells were used as negative control. The presence of the transplanted cells was verified at P60, 43 days after transplantation, after sectioning two eyes and using the fluorescence of GFP as the reporter (Figure 4A). Electroretinograms (ERGs) were recorded at P60. The b-wave amplitude of the scotopic ERG (rod response) of the eyes treated by RPE-GFP or RPE-OTX2 cells was found to be significantly higher than for the contralateral uninjected eye from $3 \times 10^{-6}$ to 10 candela cd $\times$ s/m$^2$ according to a previous report[34] (Figure 4B; Figure S2). The rod response from RPE-OTX2 transplanted eyes was higher than RPE-GFP grafted eyes. The mean of the response was almost 2-fold higher than that of RPE-GFP grafted eyes and corresponds to 29.4% of that of the wild-type, *rdy*$^{+/+}$ rats. When considering scotopic latency, the time between the stimulus and the b-wave response, RPE-OTX2 grafted eyes responded faster than eyes grafted with RPE-GFP cells at high light intensities (Figure 4C). The b-wave amplitude of the photopic ERG (cone response) was not significantly different between eyes grafted with RPE-OTX2 and those grafted with RPE-GFP cells, even if the response for RPE-OTX2 grafted eyes was higher. Nevertheless, the response of both grafted groups was significantly higher compared to that of untreated eyes (Figure 4D; Figure S2). In such conditions, the signal arises from the response of both cone photoreceptors and bipolar cells. A pure cone response was recorded by flicker ERG. In those conditions, we found that the amplitude of the response was significantly higher in transplanted eyes RPE-OTX2 compared to RPE-GFP and uninjected eyes (Figure 4E; Figure S2). When the amplitude of the protection of the cone function measure by flicker ERG is

**Figure 2. Identification of Novel OTX2 Target Genes Expressed in Retinal Pigment Epithelium**

(A) Relative *OTX2* gene expression analysis in cultured pig RPE cells infected with recombinant AAV vectors as indicated. (B) Relative *VIM* gene expression in RPE cells infected with GFP and *OTX2* (n = 4, t test, Welch correction). (C) Western blot analysis of VIM in AAV-GFP-transduced RPE cells and OTX2-transduced RPE cells (n = 3). (D) Immunocytological analysis of pig primary RPE culture at 1 and 3 weeks using anti-ACTA2 and anti-ZO-1 antibodies. (E) Relative qRT-PCR analysis of genes in AAV-OTX2- and OTX2L-transduced RPE cells. All samples were normalized to *GAPDH*. Means with SD (n = 3, Dunnett ANOVA test). (F) Predicted OTX2 binding elements in the analyzed pig promoters. Arrows indicate the position of the primers used for PCR following chromatin immunoprecipitation. (G) Chromatin immunoprecipitation in native RPE cells. −IgG, no antibodies; +IgG, unspecific to OTX2 antibodies; anti-OTX2, specific antibodies.

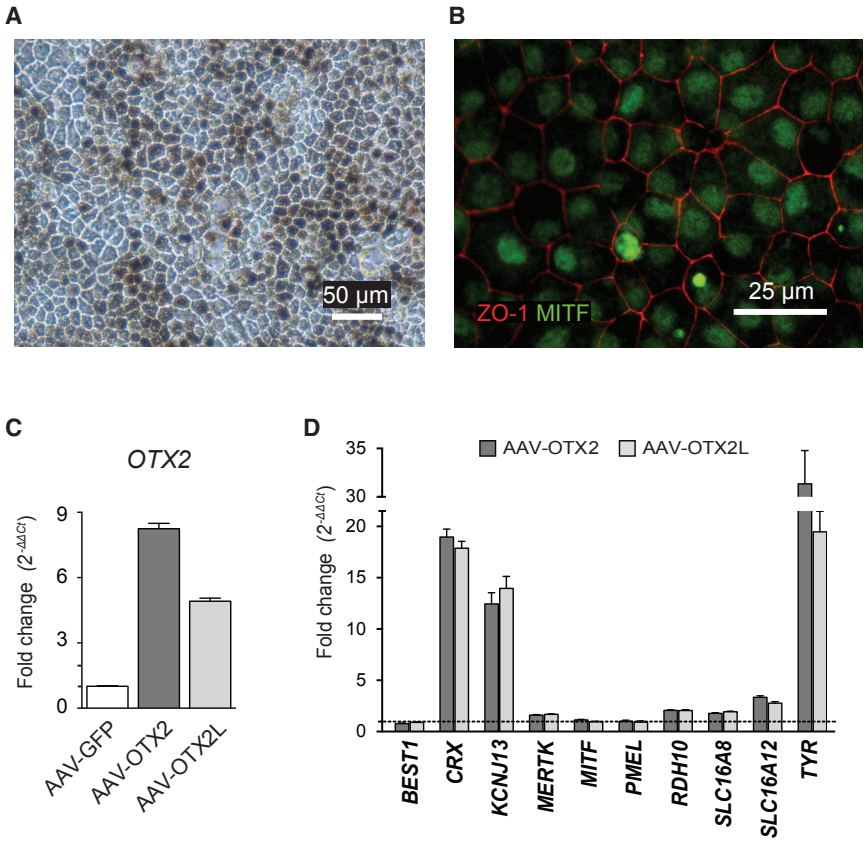


**Figure 3. OTX2 Induces the Expression of *KCNJ13*, *RDH10*, and *SLC16A8* in Human iPS-Derived RPE Cells**

(A) iPS-RPE characterization expressing melanin and cobblestone morphology. (B) iPS-RPE characterization by RPE-specific ZO-1 and MITF protein markers. (C) Relative *OTX2* gene expression analysis in iPS-RPE cells infected with recombinant AAV vectors as indicated. (D) Relative qRT-PCR analysis of genes in iPS-RPE cells in AAV-OTX2- and OTX2L-transduced cells as indicated. Because *GAPDH* expression was found to be variable in hiPS-RPE, we used *18S rRNA* for normalization. The data were compared to non-transduced cells. None of the genes showed significant change between uninfected and AAV-GFP-infected cells. All samples were normalized to *GAPDH*. Mean with SD (n = 3, ANOVA test).

analyzed (Table 3), the injection of RPE-GFP cells increases cone response by 186% and that of RPE-GFP cells by 305%, and OTX2 increases the effect of RPE transplantation by 164%. Given the average loss of cone vision of about 4% per year for patients suffering of retinitis pigmentosa, 164% would refer to 41 years of the maintenance of central vision, a medically significant situation. To examine the functional benefit of OTX2 on visual function in more detail, we performed pairwise correlations (Figures S4 and S5). The b-wave amplitude of the rod response is correlated to the cone flicker amplitide (Figure 4F) that is correlated to the b-wave amplitude of the cones (Figure 4G). The correlation between cone response measured by flicker ERG and photopic ERG suggests that the tendency observed for photopic ERG between RPE-OTX2 and RPE-GFP is real. Because rods promote cone function, the overall correlation argues for an indirect effect of OTX2-engineered RPE cells on cones via the protection of rods.[35] The efficiency of the AAV2.1 vector in delivering transgenes into pig primary RPE cells can be appreciated from the expression of the GFP reporter (Figure 4H). We did not observed any effect of OTX2 on the proliferation of RPE cells (Figure 4I).

### Grafting RPE Cells Improves Visual Behavior of the RCS Rat

The visual behavior of treated rats was accessed using a double-blind protocol at P50 by measuring optomotor head-tracking responses to rotating grating (Figure 5A).[36] Visual acuity and contrast sensitivity yield independent measures of the acuities of right and left eyes based on the unequal sensitivities of the two eyes to pattern rotation: right and left eyes are more sensitive to counter-clockwise and clockwise rotations, respectively. For visual acuity, the thickness of black and white stripes of fixed contrast is adjusted to the visual capacity of each animal. The contrast of the dark or light gray stripes of equal thickness is adjusted to measure contrast sensitivity (Figure 5B). Grafted eyes with RPE-GFP and RPE-OTX2 generated higher head-tracking response with a mean visual-acuity response at 0.492 and 0.474 cycles per degree, respectively, compared to 0.335 cycles per degree for contralateral, uninjected eyes (Figure 5C). Grafted eyes also generated an improvement in contrast sensitivity (Figure 5D): 76% and 67%, respectively, for RPE-GFP and RPE-OTX2 grafted eyes compared to 56% for uninjected eyes. No significant difference was observed between eyes transplanted with RPE-GFP and those transplanted with RPE-OTX2 cells, but both responses were almost equal that of the wild-type rats.

### Grafting RPE-OTX2 Cells Protects Rod Photoreceptors of the RCS Rats

One possible explanation for the observed results is that the transplanted cells prevent the death of rod photoreceptors, rescued rods that may prevent the secondary loss of cone function.[37,38] To investigate the protection of rods by transplantation, we measured at P60 the thickness of the ONL that is composed of 95%–97% rods in most rodents.[39] Measurements were made on the whole retina (9.5 $mm^2$). The measures were taken every 100 µm on each section by optical coherence tomography (OCT) (on average, 1,005 measurements per retina). On optical sections, the ONL is clearly identified by comparing the wild-type retina to that of the uninjected RCS rat in which this layer is absent (Figure 6A). OCT images only the central 25%–30% of the retina, so the data do not score the peripheral retina. We noticed the irregular appearance of the outer segment of the RPE interface in the eyes of transplanted RCS rats compared to the regular linear reflective band seen in wild-type

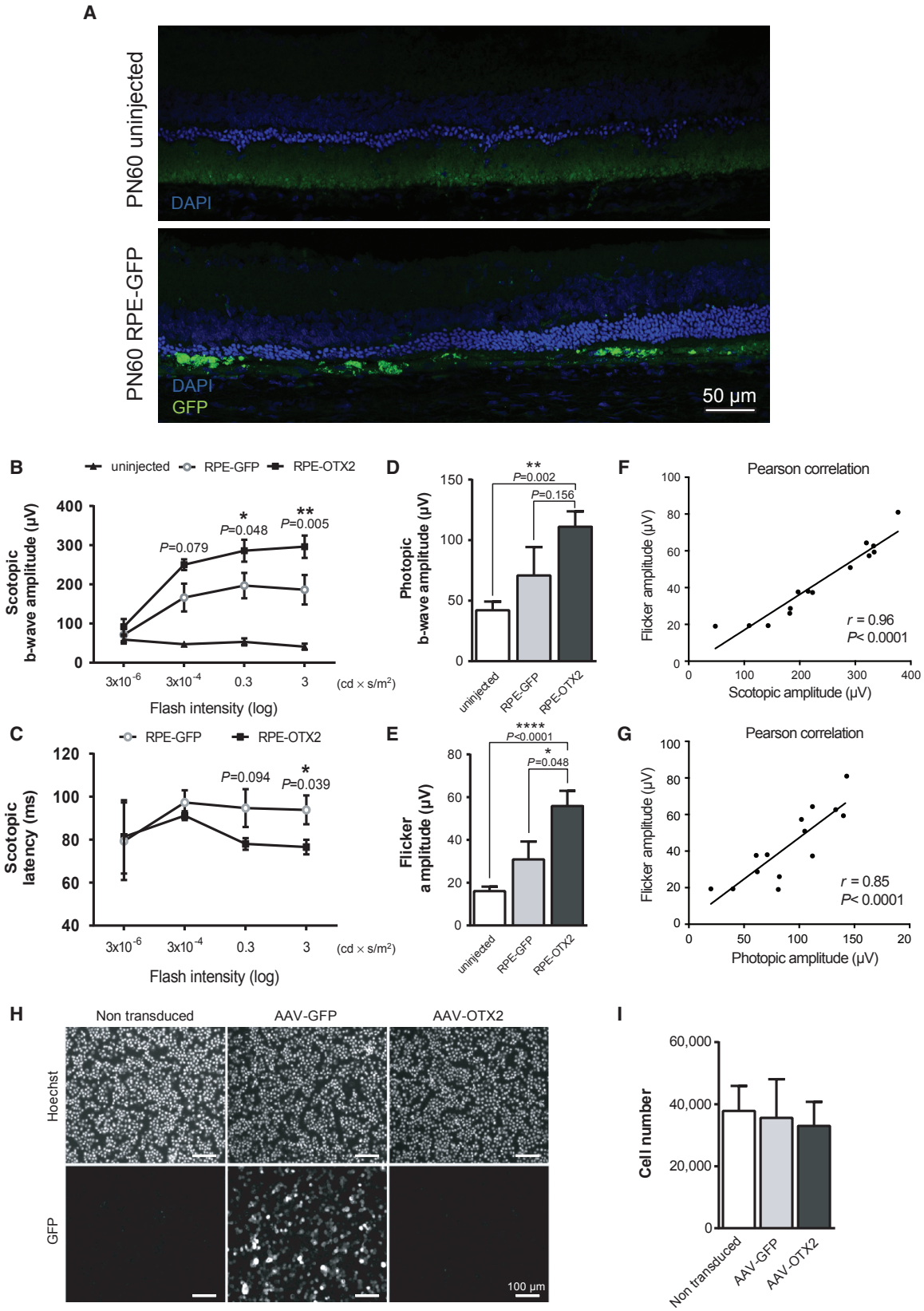


(legend on next page)

**Table 3. Comparative Analysis of the Protection of Cone Function Measured by Flicker ERG**

| | WT | Uninjected | RPE-GFP | RPE-OTX2 |
|---|---|---|---|---|
| A/B | A/B% | A/B% | A/B% | A/B% |
| WT | 100% | 6.26% | 11.66% | 19.12% |
| Uninjected | – | – | 186.32% | 305.30% |
| RPE-GFP | – | – | – | 163.87% |

eyes. This could originate from outer segment debris. We reconstructed a three-dimensional map of the retina using the mean ONL thickness at each position over the entire retinal surface. The ONL is overall thicker in the transplanted eyes, as seen by the predominance of white over the surface of the image (Figure 6B). The map shows a gradual increase in ONL thickness toward the dorsal-temporal quarter, where the cells were injected. The ONL over the whole retina is thicker in RPE-OTX2 compared to RPE-GFP grafted eyes (Figure 6C). On 95% of the retinal surface, the ONL is 6.6 μm thick for the uninjected eyes, while it is 18.5 and 25.8 μm for RPE-GFP and RPE-OTX2 eyes, respectively. The ONL thicknesses are distributed between 6 and 32 μm for RPE-GFP eyes and shifted to 13–42 μm in RPE-OTX2 eyes (Figure 6D). The bimodal aspect of both curves results from the protection of rods at the injection site, not from the presence of the transplanted cells in the subretinal space. We normalized the data over the two central sections, temporal to nasal (TN) and dorsal to ventral (DV), with the ONL thickness of the wild-type ($rdy^{+/+}$) eyes Figures 6E and 6F. We found that ONL was twice as thick in RPE-OTX2 as in RPE-GFP grafted eyes at the injection site, the dorsal-temporal quadrant of the retina. This corresponds to 40% of the thickness of the ONL in wild-type eyes, compared to 20% for RPE-GFP grafted eyes and ∼10% for untreated RCS eyes. The ONL of the transplanted RCS eyes was also thicker in the opposite part of the retina, the nasal-ventral quadrant. To test whether the benefit of OTX2 on visual function was related to rod preservation as scored by OCT, we performed pairwise correlations. The ONL thickness in the dorsal part of the retina is correlated with scotopic ERG (Figure 6G), photopic ERG (Figure 6H), and flicker ERG (Figure 6I).

The animals were sacrificed at P75, and the eyes were sectioned. Toluidine blue staining shows disorganization of the inner nuclear layer of the retina, in addition to the thinning of the ONL in the untreated RCS eyes (Figure 7A). The inner retina seems to be affected by the degeneration of rods, because it seems thinner than the wild-type control (Figure 7D). This is probably secondary to rod photoreceptor degeneration. The transplantation of RPE cells genetically modified with *Otx2* maintains the thickness of ONL compared to control and RPE-GFP, while in the uninjected eye, the ONL is almost lost and seems to prevent this secondary event to a larger extend than in RPE-GFP cells (Figures 7B and 7C). The rod nuclei in the ONL of the rats transplanted with OTX2-expressing RPE cells are more regularly organized than those of the rats treated with GFP-expressing RPE cells.

### RPE-OTX2-Modified Cells Secrete Neurotrophic Factors Protecting Cone Photoreceptors

Photoreceptor rescue distant from the injection site in RPE-GFP and RPE-OTX2 grafted eyes is indicative of a paracrine effect originating from the grafted RPE cells. We used cone-enriched primary cultures from chicken embryos to investigate the presence of neurotrophic factors in the conditioned medium of transduced RPE cells.[7] Conditioned media harvested from pig primary RPE cells infected with the AAV vectors were added to chicken retinal cultures. After 7 days of culture, the viability of the cells was scored using live and dead assay.[7] RPE cells naturally secrete protective molecules. Nevertheless, compared to RPE-GFP, RPE-OTX2 induces cell survival to a larger extent (Figure 8A). The conditioned medium from OTX2-transduced pig RPE cells promotes 3-fold greater increases in cell survival than does that from the negative control (conditioned medium [CDM]) and 1.5-fold greater increases when compared to medium from GFP-transduced RPE cells. The morphology of the cone cells was elongated with neuritic extensions in the presence of conditioned medium from AAV-OTX2-transduced RPE cells compared to the round cells in the negative control (CDM) and in the presence of conditioned medium from GFP-transduced RPE cells (Figure 8B). qRT-PCR analysis of RNA isolated from RPE cells transduced with OTX2 shows that the expression of ciliary neurotrophic factor (CNTF) is induced by OTX2 while that of brain-derived neurotrophic factor (BDNF) remains unchanged (Figure 8C). The conditioned medium of RPE cells transduced by OTX2 was shown to contain less than 1 ng/mL of CNTF, the detection limit of the ELISA system used. Using western blot on whole-cell extracts of these cells, no CNTF signal could be detected (Figure 8D). Tested at 1 mg/mL, recombinant CNTF has no protective effect on cones using the cone-enriched culture system (Figure 8E). Because CNTF has previously been reported to protect photoreceptors,[40]

**Figure 4. Genetically Modified RPE Cells Overexpressing OTX2 Rescue Photoreceptor Function in RCS Rats**

(A) Immunofluorescence detection of GFP-positive pig RPE cells in subretinal space 47 days post-transplantation. (B) Scotopic electroretinogram (ERG) comparison between untreated eyes and grafted eyes with RPE-GFP and RPE-OTX2 cells. The p values correspond to RPE-OTX2 versus RPE-GFP. (C) Comparison of scotopic time latency in RPE-GFP and RPE-OTX2 grafted eyes. The p values correspond to RPE-OTX2 versus RPE-GFP. (D) Photopic ERG responses. Comparison in untreated (white bar), RPE-GFP (light gray), and RPE-OTX2 (dark gray) grafted eyes. Points are shown as mean with SEM, n = 7. (E) Flicker ERG comparison in untreated (white bar), RPE-GFP (light gray), and RPE-OTX2 (dark gray) grafted eyes. Points are shown as mean with SEM, n = 7. (F) Pairwise correlation between scotopic ERG and cone flicker ERG. (G) Pairwise correlation between photopic ERG and flicker ERG. (H) Cytological analysis of pig RPE cells infected or not with recombinant AAV vectors as indicated. (I) Quantification of the number of cells labeled with Hoechst. For statistical analyses, scotopic ERG, Bonferroni ANOVA test; grafted versus uninjected eyes, Wilcoxon matched pairs; RPE-GFP versus RPE-OTX2, unpaired Kolmogorov-Smirnov test.

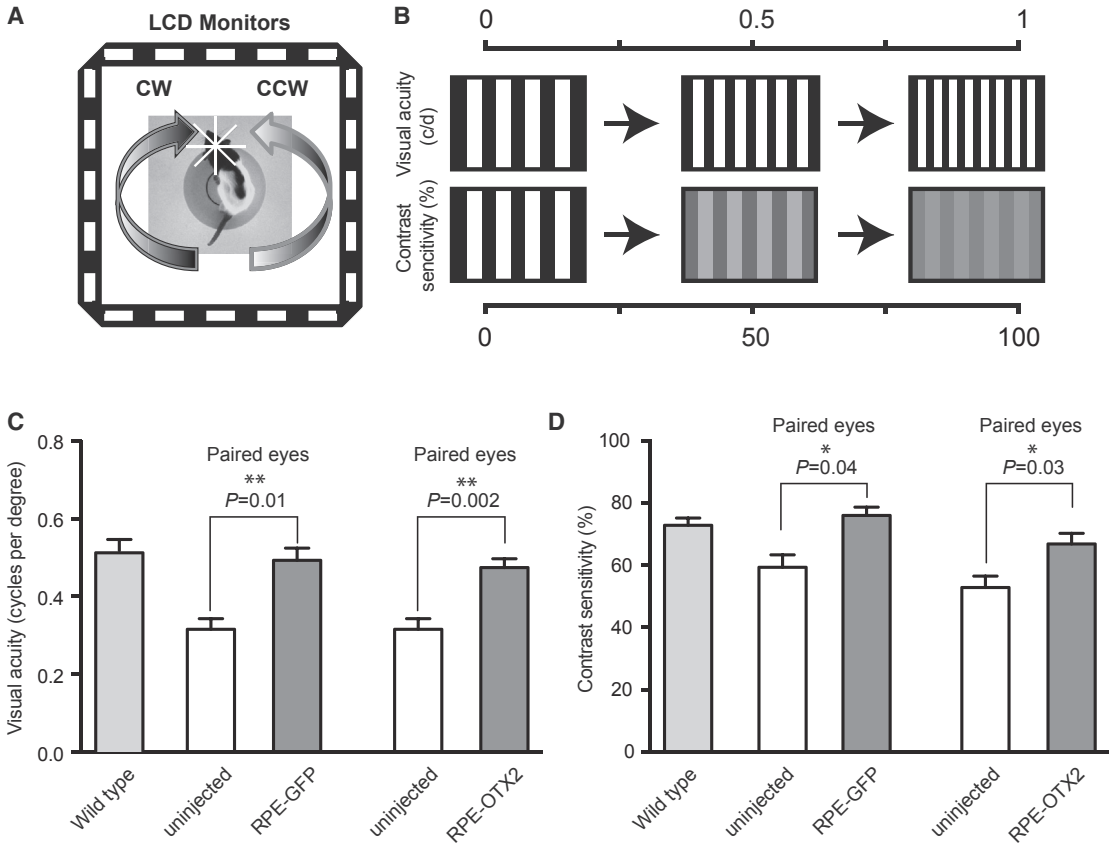


**Figure 5. RPE Transplantation Improves Visual Behavior in RCS Rats**

(A) Schematic representation of the optokinetic chamber. (B) Optometry setup. (C) Visual acuity. (D) Contrast sensitivity comparisons. Mean with SEM (n = 7, Wilcoxon matched pairs t test). CW, clockwise rotation (left eye drives response); CCW, counter-clockwise rotation (right eye drives response).

the effect of transplantation may be partly mediated by CNTF. A possible molecular network connecting the expression of OTX2 and CNTF was revealed by measuring the expression of their respective mRNA in the RPE of the RCS rats at P15, before the initiation of rod degeneration triggered by Mertk loss-of-function mutation (Figure 8F). Even if the mechanism of protection by OTX2 remains elusive, the transcription activation property of OTX2 is likely to be involved, because its major target gene, CRX, is elevated in the eye of RCS rats transplanted with OTX2-genetically modified pig RPE cells (Figure 8G).

## DISCUSSION

The present study shows the benefit of OTX2 on the outcome of RPE transplantation in a model of inherited retinal disorder, the RCS rat. The protection of rods as shown by measuring the thickness of the ONL is correlated with the measurement of rod function by ERG. The absence of difference between OTX2-treated eyes and their negative control, GFP, in visual behavior assays is surprising but may result from the lack of sensitivity of visual tests in nocturnal animals, such as the rat. Alternatively, because visual acuity can be measured in patients with no ERG recordable for years,[41] the optomotor test cannot distinguish the effect of RPE-OTX2. There is no sharp difference between the performance of the wild-type and that of the treated dystrophic eyes at P50 (Figure 5). Most likely, after transplantation, the effect of OTX2 could have been distinguished from that of sole transplantation. ERG, especially flicker ERG, shows improved cone function in the presence of RPE-OTX2.

Even if the protective effect of OTX2 cannot be attributed to an inhibition of the epithelial to mesenchymal transition, the transcription factor OTX2 directly enhances the activity of promoters of genes downregulated during in vitro dedifferentiation of primary RPE cells, which suggests that the protective activity of OTX2 for the visual function of the RCS rat is linked to OTX2-regulated genes involved in RPE differentiation. The spread of the effect observed distant from the site of injection of the grafted cells implies that rod protection is unlikely to result from the restoration of outer segment phagocytosis by the transplanted RPE cells that remain localized at the injection site. Our results are consistent with the role of *Otx2* in the adult mouse RPE, because the conditional knockout of *Otx2* leads to disruption of photoreceptor-RPE

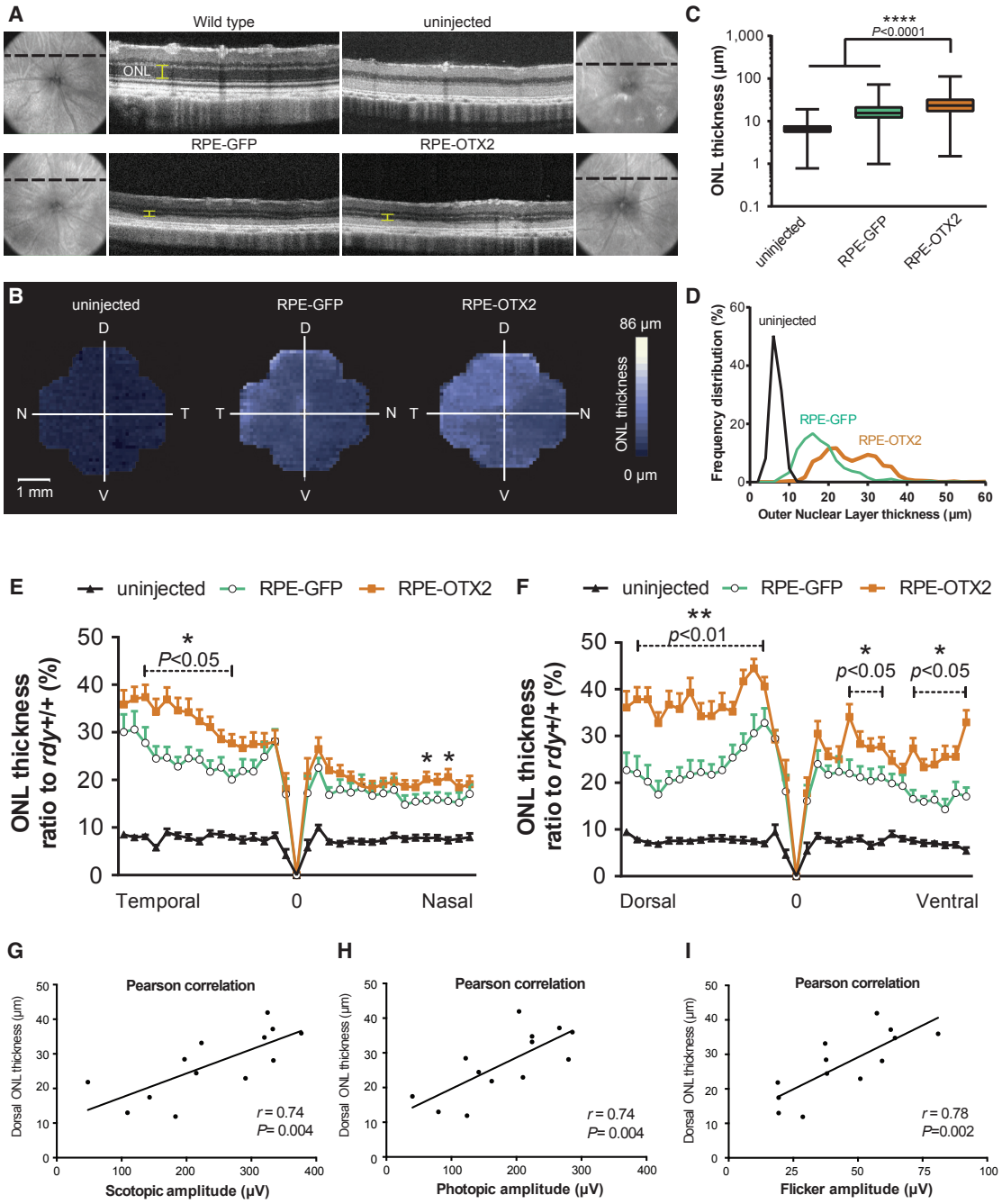


**Figure 6. Genetically Modified RPE Cells Overexpressing OTX2 Rescue Outer Nuclear Layer in RCS Rats**

(A) OCT representative sections in wild-type, dystrophic untreated, RPE-GFP grafted, and RPE-OTX2 grafted eyes. (B) 3D representation of the mean ONL thickness in dystrophic uninjected, RPE-GFP grafted, and RPE-OTX2 grafted eyes. (C) ONL thickness comparisons between uninjected, RPE-GFP grafted, and RPE-OTX2 grafted eyes, mean with minimum and maximum (Mann-Whitney test). (D) ONL thickness frequency distribution in uninjected, RPE-GFP grafted, and RPE-OTX2 grafted eyes. (E and F) Rational ONL thickness to wild-type comparison between temporal to dorsal (E) and dorsal to ventral (F) axes. The p values correspond to the comparison between RPE-OTX2 and RPE-GFP. (G) Pairwise correlation between ONL thickness and scotopic ERG. (H) Pairwise correlation between ONL thickness and photopic ERG. (I) Pairwise correlation between ONL thickness and flicker ERG. Mean with SEM (Wilcoxon matched pairs t test). OCT, optical coherence tomography; T, temporal; N, nasal; D, dorsal; V, ventral.

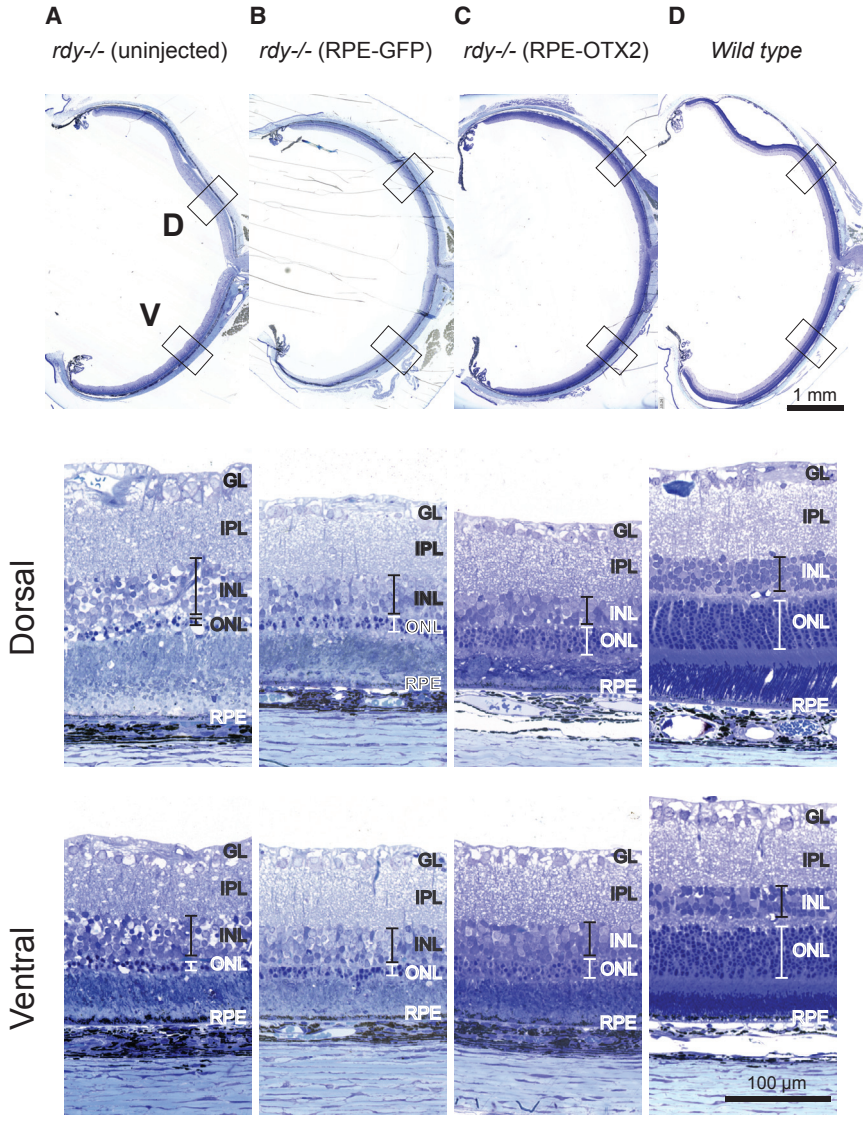


**Figure 7. OTX2-Grafted Cells Maintain Photoreceptor Rescue in Later Stages of Degeneration**

(A–D) Toluidine blue-stained sections. Photoreceptor debris is located in the subretinal space in the dystrophic uninjected eye (A), but no longer after transplantation (B and C) or in the wild-type retina (D).

adhesion and photoreceptor degeneration.[42,43] We showed that OTX2 induces the expression of 9 of 27 genes, which are downregulated following in vitro dedifferentiation: *CACNB2*, *CRX*, *KCNJ13*, *KRT18*, *RDH10*, *SLC16A8*, *SCL16A12*, *TYR*, and *TYRP1* (Table 2). Among them, *RDH10* is acting in the retinoid cycle, and three other genes (*CRX*, *KCNJ13*, and *SLC16A8*) have been involved in retinal diseases. OTX2 and CRX are the key homeoproteins that regulate the initial specification of the photoreceptor lineage.[44] CRX has even been reported to be expressed in the RPE.[45] KCNJ13 (KIR7.1) is a potassium channel located in the apical membrane in the RPE[46,47] and is responsible, together with chloride channels, for the transport of water from the subretinal space to the choroid, decreasing the risk for retinal detachment. The disruption of the lactate transporter gene *Slc16a8* leads to an accumulation of lactate in the outer retina and to photoreceptor dysfunction.[48] A risk allele within the *SLC16A8* gene is predisposing for age-related macular degeneration, a disease that involves dysfunction of the RPE.[49] The protection of photoreceptors of the RCS rats may result from a combination of effects, including trophic interaction between the grafted RPE cells and the photoreceptors from the host. In addition to a possible hypothetic effect on the visual cycle, we highlight the increase in expression of membrane proteins of the RPE that, as KCNJ13, increases photoreceptor-RPE cellular interactions or, as SLC16A8, detoxifies the subretinal space.[48] Detoxification generates a non-cell autonomous effect as one expects for the action of trophic factors. Furthermore, cells incubated with conditioned medium from RPE-OTX2 cells showed elongated cone morphology compared to round cells found in controls. The nature of these secreted factors remains uncertain. CNTF was shown to promote the regeneration of outer segments in degenerating cones.[50] CNTF mRNA is upregulated, but no protein could be detected in cell extract and in the conditioned medium of OTX2-transduced RPE cells. Given the reported negative effect of CNTF on electrical response in the mouse retina, the effect observed by grafting cells overexpressing OTX2 might be unrelated to the upregulation of CNTF.[51] Alternatively, we could not rule out that the effect on cones is mediated by OTX2, because it has been shown to mediate paracrine effects in the retina.[52]

In addition to retinitis pigmentosa, other retinal diseases with loss of RPE cells, such as Best's disease, would require treatment by transplanting healthy RPE cells. Patients undergoing choroidal neovascularization removal with autologous transplantation of RPE reached significantly better reading acuity than control subjects.[53] In recent years, several clinical trials using transplantation of RPE cells have been made to treated age-related macular degeneration.[53,54] Attempts have been made to extend the lifespan of the RPE cells or to transduce these cells with trophic factor before transplantation without success.[55,56] The effect of OTX2 is probably mediated through the maintenance of a proper differentiation status of the grafted cells, which is also relevant in the field of iPSC transplantation (Figure 3). The expression of desirable markers for each cell type after iPSC

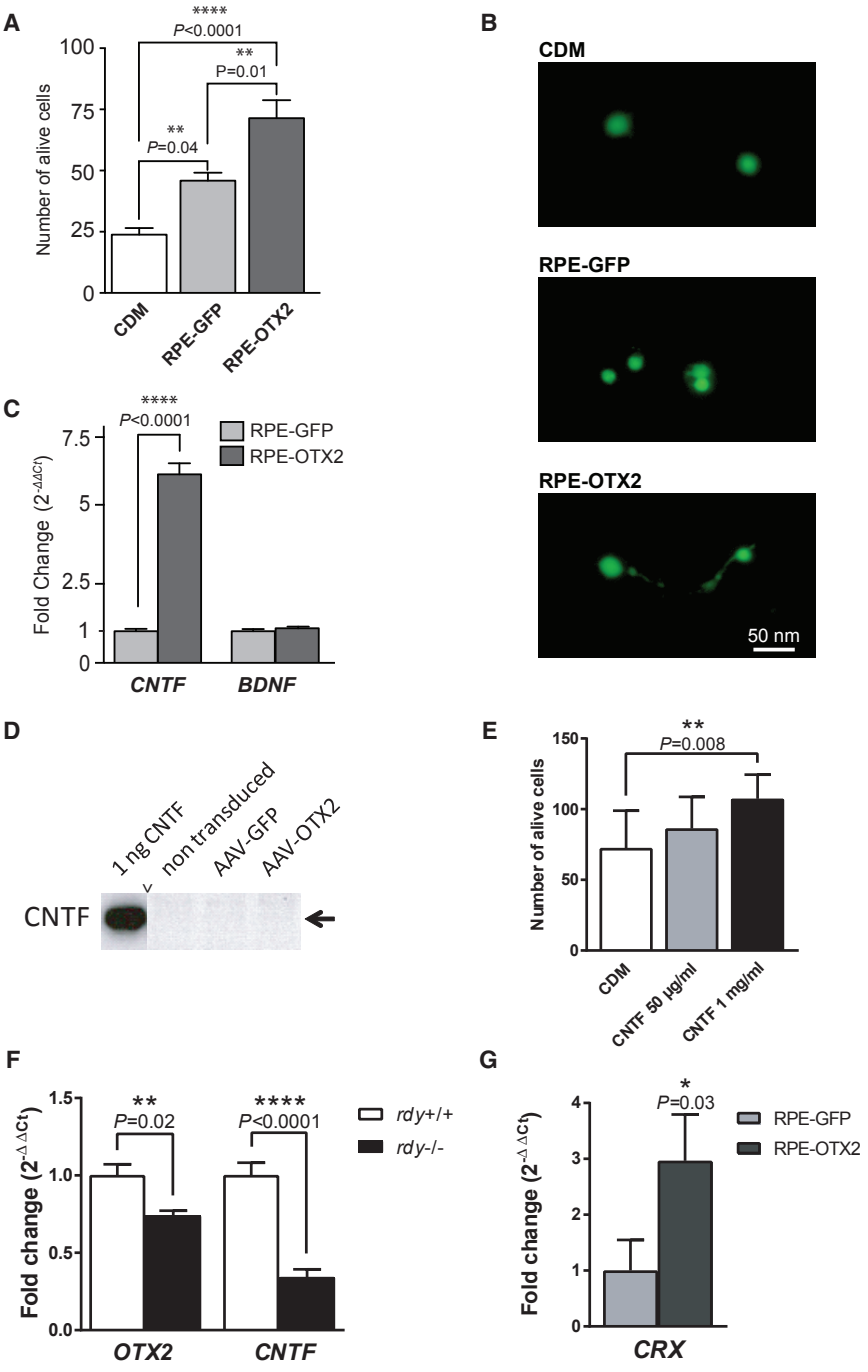


**Figure 8. RPE-OTX2 Cells Secrete Neurotrophic Factors that Promote Cone Rescue**

(A) Cone photoreceptor survival by supernatant from AAV-GFP- and OTX2-transduced pig primary RPE cells. CDM represents conditioned non-cell incubated medium. Mean with SEM (n = 6, Holm-Sidak multiple comparison ANOVA). (B) Morphology of the cone cells after incubation with supernatant from RPE-GFP, OTX2, and CDM. Cells are labeled with the viability dye Calcein-AM. (C) Relative qRT-PCR expression of *CNTF* and *BDNF* in AAV-OTX2-transduced cells as indicated. (D) Western blot of RPE cells transduced with recombinant AAV vectors as indicated. Pig CNTF was used as positive control. (E) Absence of protection of cones from the cone-enriched cultures by purified CNTF. (F) Quantification of *Otx2* and *Cntf* mRNA in the RPE of the RCS rat at P15. (G) Increase in the expression of CRX mRNA in the eye of RCS rat transplanted by OTX2-modified pig RPE cells. Data were normalized to *GAPDH*. Mean with SD (n = 3, ANOVA test).

differentiation is usually not sufficient to obtain a therapeutic effect; the expression of these genes should also approximate the level of healthy cells in living tissue, which OTX2 might help to achieve.

## MATERIALS AND METHODS

### Animals

Pigmented dystrophic RCS ($rdy^{-/-}$, $p^{+}$) rats were maintained in the animal facility at Institute de la Vision, Paris. Adult (male and female) recipient animals were at P18 at transplantation. All experiments have been conducted in accordance with the policies on the use of animals and humans in neuroscience research, revised and approved by the ethics committee in animal experiment Charles Darwin for the use of animals in ophthalmic and vision research. Animals were kept on a standard 12/12 hr light/dark cycle, and all assessments of visual function were conducted in the first 8 hr of the light phase. All transplanted animals were maintained on 210 mg/L of oral cyclosporine A (Merck Millipore 239835) administered in the drinking water from day 2 before transplantation until the day they were sacrificed.

### RNA Purification

Post-mortal human retina samples with or without retinal detachment, control samples, and pig primary RPE cells, native or cultured, were placed in guanidine hydrochloride solution, and total RNA was purified using the cesium chloride ($CsCl_2$) method.[57] Briefly, tissue or cell samples were homogenized in 6 M guanidine-HCl using polytron (Kimematica PT2100). After homogenization, samples were incubated for 10 min at room temperature (RT) with 2 M potassium acetate (pH 5.0) followed by 10 min of centrifugation at 5,000 rpm and 20°C. The supernatant was mixed with 5.3 mL of 100 mM Tris-HCl (pH 8.0), 1% N-laurylsarcosine, and 3.2 g of $CsCl_2$ and was transferred on top of 1.8 mL of CsCl/EDTA in polyallomer ultracentrifugation tubes (Rotor SW 41 TI, Beckman) to create a CsCl gradient. Samples were centrifuged using Optima LE80k (Beckman) at 35,000 rpm for 24 hr at 20°C. The pellet was resuspended in 150 µL of 10 mM Tris-HCl (pH 7.5),

1 mM EDTA, and 0.1% SDS. Total RNA was purified using phenol-chloroform extraction and resuspended in diethylpyrocarbonate (DEPC) water. Denaturing gel electrophoresis assessed RNA integrity.

### Reverse Transcription and Real-Time PCR

First-stranded cDNA was synthesized from 1 μg of total RNA using random primers (Promega) and Superscript II reverse transcriptase (Invitrogen), following manufacturer instructions. Briefly, 1 μg of total RNA, after DNase I (Life Technologies 18068-015) treatment and inactivation at 65°C for 5 min, was mixed with 5 U RNasin Plus (Promega), 100 ng of random primers (Promega), 10 mM dinucleotide triphosphate (dNTP) (Invitrogen), 0.1 M DTT, and 4 U reverse transcriptase enzyme. Samples were incubated at 42°C for 50 min, and enzymatic reaction was inactivated by incubation at 72°C for 15 min. The endogenous expression of genes in human samples, human-induced pluripotent stem cell (hiPSC)-derived RPE (hiPS-RPE) cells, and primary pig RPE cells were quantified by real-time RT-PCR in using gene-specific primers (Table S1). Primers efficiency was determined before the analysis, and only primers with an efficiency ranking from 90% to 110% and $r \approx 1$ were used for the quantitative analysis. 10 ng of cDNA was mixed with 0.1 mM forward-reverse primer mix and 1× power SYBR Green (Invitrogen 4367659). Amplification and analysis of the amplitude (cycle threshold, Ct) was performed using the 7500 Real-Time PCR System (Applied Biosystems) and briefly using the following sections: 1st, 1 cycle at 95°C; 2nd, 40 cycles of 15 s at 95°C, followed by 20 s at 60°C; and 3rd, 1 cycle of 1 min at 95°C, 30 s at 55°C, and 30 s at 95°C. The expression of each gene was normalized by the expression of housekeeping genes (*GAPDH* or *18S rRNA*) using the ΔCt formula, following manufacturer instructions. For analysis of human retinal detachment and gene screening in hiPS-RPE and pig primary RPE cells, glyceraldehyde-3-phosphate dehydrogenase (*GAPDH*) was used as the housekeeping gene. For characterization of hiPS-RPE, *18S rRNA* was used as the housekeeping gene. For comparative analysis, the results were calculated using the ΔΔCt formula, following manufacturer instructions, and fold expression was presented as $2^{-\Delta Ct}$ and/or $2^{-\Delta\Delta Ct}$.

### Plasmid Construction

The vector plasmid pAAV2-CMV-EGFP, carrying the AAV2 inverted terminal repeat (ITR) sequences and the transgene cassette encoding EGFP under control of a cytomegalovirus (CMV) promoter, is a gift of Dr. Bennett. The plasmids pAAV2-CMV-*Otx2* and pAAV2-CMV-*Otx2L* (splicing variant) were constructed by replacing the EGFP in the plasmid pAAV2-CMV-EGFP with the coding DNA sequence (CDS) of rat *Otx2* and *Otx2L* in NotI (5′) and BamHI (3′) restriction enzymes sights. The rat *Otx2* and *Otx2L* fragments were amplified from the plasmids LA0ACA 144YK13CM1 and LA0ACA6YL17.CONTIG, respectively (http://kbass.institut-vision.org/KBaSS/), via high-fidelity PCR using the forward primer 5′-GTGTCCAGGCGGCCGCAAAAATGATGTCT TATCTAAA and reverse primer 5′-AATCGGATCCCGATATCT CACAAAACCTGGAATTTCCA. The helper plasmid (pHelper) providing the three-adenoviral helper genes VA, E4, and E2A, as well the plasmid pLT-RC02 encoding for the proteins of an AAV1 capsid, are a gift of Dr. Bemelmans.

### Production of the AAV2.1 Viruses

The AAV2 vectors with transgene cassettes encoding for GFP or *Otx2* and *Otx2L* splicing variants under control of the CMV promoter were packaged into an AAV1 capsid. Briefly, $15 \times 10^6$ HEK293 cells were triple transfected with 12 μg of pHelper, 10 μg of pLT-RC02, and 6 μg of pAAV2-CMV-EGFP, pAAV2-CMV-*Otx2*, or pAAV2-CMV-*Otx2L*. These constructs were mixed with 120 μL and 1 μg/μL of polyethylenimine (PEI) and 500 μL of DMEM. 48 hr after transfection, cells were harvested. Supernatant was incubated for 2 hr at 4°C with 1× polyethylene glycol (PEG) solution (8% PEG, 5M NaCl). Cells were lyses by 3 cycles of freezing and thawing resuspended in lysis buffer (0.15 M NaCl, 50 mM Tris-HCl [pH 8.5]). Cell lysate was combined with PEG pellet, and viral particles were collected by iodixanol gradient (15%, 25%, 40%, and 60%) and centrifuged as described.[58] The 40% fraction containing the AAVs was collected and purified by 1× PBS, 0.001% pluronic. Viral particles were stored in PBS, 0.001% pluronic, at 4°C. Titers were determined by quantification using real-time PCR using the primers 5′-GGA ACCCCTAGTGATGGAGTT and 3′-CGGCCTCAGTGAGCGA that target the ITR sequence and are expressed as viral genomes per milliliter.

### Human-Induced Pluripotent Stem Cell-Derived RPE Cells

The integration-free human iPSC line, hiPSC-2, was generated from adult human dermal fibroblast. hiPSC-2 were maintained on a mitomycin C-inactivated mouse embryonic fibroblast feeder layer (Zenith Biotech) in ReproStem medium (ReproCELL) with 10 ng/mL of human recombinant basic fibroblast growth factor (FGF2) (PeproTech). Cells were incubated at 37°C in standard 5% $CO_2$/95% air and mechanically passaged once a week. Human iPS-RPE cells were obtained by differentiation of confluent hiPSC-2 as described.[59] Patches of pigmented cells were mechanically dissected and expanded on gelatin-coated culture dishes, noted as passage 0, to reach confluence. Human iPS-RPE cells were characterized by their morphology, pigment expression, and immunocytochemistry detecting RPE-specific markers (MITF and ZO-1) at passage 0. Expression of RPE gene markers was determined using qRT-PCR and the primers listed in Table S1. Human iPSC-derived RPE cells can be propagated for up to four passages while retaining their RPE morphology. Gene expression studies were performed on cells at passage 1.

### Pig RPE Primary Culture

Pig eyes were collected from three breeds (Pietrain, Large White, and Landrace), and were obtained from an authorized slaughterhouse (Abattoir Guy Harang, Houdan, France). The eyes were disinfected for 3 min in 95% ethanol and transferred in $CO_2$-independent medium (Invitrogen). A small incision was done using a needle at the ora serrata (3 mm of the cornea), and the eye was cut around the cornea, which was removed afterward. The eye globe was cleaned from the lens, vitreous, and neural retina. RPE or choroid eyecups

were washed twice with PBS, filled with trypsin-EDTA 0.25% to up to two-thirds of the eyecups, and incubated at 37°C for 1 hr and 40 min. RPE cells were collected by gentle up and down pipetting and transferred into DMEM containing 20% fetal bovine serum (FBS) and 10 μg/mL of gentamicin. RPE cells from 11 eyes were pooled together and plated into five 10 $cm^2$ dishes in the same medium. The culture medium was changed on day 1 and day 4. By days 5–6, the cultures became confluent and showed a cobblestone-like appearance characteristic of RPE cells.

#### Chicken Cone Photoreceptor-Enriched Culture

Eyes from chicken embryos at stage 29 were dissected and cleaned in 1× PBS, and the eyes were transferred in $CO_2$-independent medium. Using dissecting instruments, neural retina was isolated and carefully cleaned from the cornea, vitreous, lens, and any other remaining tissue. The neural retina was transferred into fresh $CO_2$-independent medium and dissociated in small pieces with the help of dissecting tools. The pieces were transferred into a new tube. Trypsin-EDTA 0.25% dissociation at 37°C for 20 min followed centrifugation. Trypsin reaction was stopped by adding medium M199 containing 10% FBS followed by centrifugation. Photoreceptor progenitors were incubated with CDM (50% M199, Life Technologies 11150-059; 50% DMEM) supplemented with 5 μg/mL of insulin, 5 μg/mL of sodium selenite, 16.1 μg/mL of putrescine, 0.63 μg/mL of progesterone, 100 μg/m of prostaglandin, 375 μg/mL of taurine, 2.56 μg/mL of cytidine-5′-diphosphocholine, 1.28 μg/mL of cytidine-5′-diphosphate ethanolamine, 0.2 μg/mL of hydrocortisone, 0.02 μg/mL of tri-iodotyrosine, 110 μg/mL of sodium pyruvate, and 100 μg/mL of linoleic acid.

#### In Vitro Transduction

For in vitro transduction, pig primary RPE and hiPS-derived RPE cells were seeded in 12-well plates, $12 \times 10^6$ cells/well, in DMEM containing 10% FBS. The following day, cells were washed with 1× PBS and incubated for 5 hr with 300 μL of DMEM containing $6 \times 10^{10}$ viral particles (AAV2.1-GFP or AAV2.1-*Otx2v* splice variants). After 5 hr of incubation, the medium was adjusted to 10% FBS and 10 μg/mL of gentamicin. The cells were incubated for 10 days at 37°C in 5% $CO_2$. The medium was changed once at day 5. For transplantation studies, the pig primary RPE cells were incubated for 7 days with the virus used for transduction.

#### Western Blot and Immunocytochemistry

Western blot protocol was done as described in Léveillard et al.[7] Briefly, transduced pig primary RPE cells were lysed in 50 mM Tris-HCl (pH 7.5), 1 mM EDTA, 1 mM DTT, 50 mg/mL of tosyl-L-lysyl-chloromethane hydrochloride (TLCK; Sigma), 1× protease inhibitors (Sigma), and 10 μg/mL of Triton X-100, followed by sonication. Antibodies used are as follows: anti-OTX2 (R&D Systems AF1979, 1/1,500), anti-ACTB (1/500), and anti-CNTF (EMELCA Bioscience 251634, 1/250). Immunolabeling of the hiPS-RPE monolayer at passage 0 after 45 days in culture was done for ZO-1 and MITF. Briefly, cells were fixed for 10 min in 4% formaldehyde followed by 3 washes with 1× PBS. Blocking was performed for 1 hr at RT with PBS, 0.2% gelatin, and 0.25% Triton X-100 and followed by overnight incubation at 4°C with the primary antibody. The antibodies used are as follows: anti-ZO-1 (Life Technologies 61-7300, 1/250) and anti-MITF (clone D5, Dako M3621, 1/200). Slides were washed three times in PBS with 0.1% Tween 20 and then incubated for 1 hr at RT with the appropriate secondary antibody conjugated with Alexa Fluor 488 or 594 (Life Technologies, 1/600) and DAPI (1/1,000). Fluorescent staining signals were captured with a DM6000 microscope (Leica Microsystems) equipped with a charge-coupled device (CCD) CoolSNAP-HQ camera (Roper Scientific) or using an Olympus FV1000 confocal microscope equipped with 405, 488, and 543 nm lasers. Confocal images were acquired using a 1.55 or 0.46 μm step size and corresponded to the projection of 4–8 optical sections. Sandwich pig CNTF ELISA (LSBio LS-F6243) was used, following manufacturer instructions. Pig CNTF provided in the kit was used as positive control in western blot.

#### ChIP

Chromatin immunoprecipitation (ChIP) was performed as described previously.[60–62] Briefly, fresh RPE cells were dissected from 6 pig eyes and pooled together. RPE was cross-linked with ice-cold 4% formaldehyde in PBS for 30 min, rinsed in PBS, and sonicated (Vibra Cell) in lysis buffer (1% SDS, 10 mM EDTA, 50 mM Tris-HCl [pH 8.0]) and protease inhibitors (Sigma) to an average DNA size of 800 base pairs (bp). The sonicated sample was centrifuged at 15,000 rpm for 10 min at 4°C, and the supernatant was pre-cleared with glutathione Sepharose (G-sepharose) beads (Fisher PI-20399) for 1 hr at RT. Aliquots of 100 μL was diluted to 1.5 mL with dilution buffer (1% Triton X-100, 2 mM EDTA, 150 mM NaCl, 20 mM Tris-HCl [pH 8.0]) and subdivided into three reactions that were incubated for 1 hr at RT with (1) no antibody, (2) 2.5 μg of anti-rabbit antibodies (Jackson Laboratory 111-035-045), and (3) anti-OTX2 antibodies (Millipore ab9566). Samples were centrifuged at 15,000 rpm for 10 min at 20°C, and the supernatant was mixed with 15 μL of protein G-Sepharose beads, 150 μg of ultrapure salmon sperm DNA (Invitrogen 15632-011), and 150 μg of yeast tRNA (Invitrogen 15401-011) and incubated for 1 hr and 30 min at RT. Precipitates were washed sequentially for 10 min at RT with TSEI (0.1% SDS, 1% Triton X-100, 2 mM EDTA, 20 mM Tris-HCl [pH 8.0], 150 mM NaCl), 4 times with TSEII (0.1% SDS, 1% Triton X-100, 2 mM EDTA, 20 mM Tris-HCl [pH 8.0], 500 mM NaCl), once with buffer III (0.25 M LiCl [pH 8.0], 1% Nonidet P-40, 1% deoxycholate, 1 mM EDTA, 10 mM Tris-HCl [pH 8.0]), and finally three times with TE buffer (10 mM Tris-HCl [pH 8.0], 1 mM EDTA). Samples were eluted, and cross-links were cleared by overnight incubation at 65°C in 100 μL of elution buffer (1% SDS, 0.1 M $NaHCO_3$). DNA fragments were purified by phenol-chloroform extraction and resuspended in 70 μL of TE buffer. Semi-qPCR was used to amplify 2 μL of immunoprecipitated material. PCR reaction was performed in 25 μL at 94°C for 3 min, 40 cycles (94°C/15 s, 60°C/15 s, and 72°C/30 s), followed by 72°C for 3 min. The primers used were designed to amplify fragments into the promoter genes: *KCNJ13*, forward 5′-GCAGGCCTTC CATGATTTTA and reverse 5′-TGAGCTGTCAGATGGCTTTG;

*SLC16A12*, forward 5′-TGCCTGTCCCACTAGGAAGT and reverse 5′-GCATCATTTGCCATGTGACT; *RDH10*, forward 5′-GGCAAC AAGTCCCACCTAAA and reverse 5′-GTTTACTTGGTGGGGG AGGT; *TYRP1*, forward 5′-CCAATTTGCAGGGAACAAAT and reverse 5′-TGCCTTAAATTGCCTTCTCAA; and *HGB*, forward 5′-GAACGTCAGGATTCCCTTGA and reverse 5′-CCATTGGGA GCTTCCTTGTA.

### Retinal Pigment Cell Preparation and Transplantation

Transduced primary pig RPE cells with AAV2.1-GFP or AAV2.1-OTX2 were incubated for 1 week as previously described before transplantation. Cells were washed twice with HBSS (Hank's balanced salt solution, calcium, magnesium, no phenol red) (Invitrogen) and dissociated with trypsin-EDTA 0.05%. RPE cells were collected by gentle pipetting and transferred into HBSS containing 20% FBS. The resulting pellet of cells was resuspended at a concentration of 25,000 cells/μL in HBSS. Surgery was performed under direct ophthalmoscopy through an operating microscope (Figure S6). A blind protocol was employed in which the surgeon was not informed about the identity (RPE-GFP or RPE-OTX2) of cells injected into each rat at P18. GFP-expressing cells cannot be identified before surgery in this setting. Recipient rats were anaesthetized with a single intra-peritoneal injection with a mixture of ketamine (100 mg/kg) and xylazine (10 mg/kg) a minimum 10 min before surgery. A blunt-ended 30 gauge Hamilton needle attached to a Hamilton syringe (10 μL, Model 1701 RN SYR, NDL Sold) was inserted tangentially through the sclera and RPE into the subretinal space. Cell suspensions were slowly injected, with 50,000 cells per eye. Throughout the procedure, eye dehydration was prevented by regular instillation of sodium chloride drops. After surgery, both treated and untreated eyes were kipped closed for dehydration and destruction of the cornea. Rats were kept in chambers at 35°C until recovery from anesthesia.

### Optomotor Response

Contrast sensitivities and visual acuities of treated and untreated eyes were measured by optometry using the OptoMotry 1.77 system (Cerebral Mechanics, Canada), by observing the optomotor responses of rats to rotating sinusoidal gratings.[36,63,64] Briefly, rats reflexively respond to rotating vertical gratings by moving their head in the direction of grating rotation. The protocol used yields independent measures of the acuities of right and left eyes based on the unequal sensitivities of the two eyes to pattern rotation: right and left eyes are most sensitive to counter-clockwise and clockwise rotations, respectively. A double-blind procedure was employed, in which the observer was masked to the direction of pattern rotation, to which eye received the treatment, and to which eye received RPE-GFP or RPE-OTX2 cells. Briefly, each rat at P50 was placed on a pedestal located in the center of four inward-facing liquid crystal display (LCD) computer monitor screens and was observed by an overhead infrared video camera with an infrared light source. Once the rat became accustomed to the pedestal, a 7 s trial was initiated by presenting the rat with a sinusoidal striped pattern that rotates either clockwise or counter-clockwise, as determined randomly by the OptoMotry software. Involuntary reflex head-tracking responses are driven by the left eye (clockwise rotations) and right eye (counter-clockwise rotations), respectively. Contrast sensitivity was measured at a spatial frequency of 0.042 cycles per degree and at a speed of rotation of 0.5 Hz. To assess visual acuity, gratings had a constant contrast of 100% and initial stimulus was 0.042 cycles per degree. Using a staircase paradigm, the program converges to measures of the acuities or contrast sensitivity of both eyes, defined as the spatial frequency or percent contrast yielding $\geq$70% correct observer responses. Acuity was defined as the highest spatial frequency yielding a threshold response. Similarly, contrast sensitivity was defined as 100 divided by the lowest percent contrast yielding a threshold response. While this protocol permits the separation of right and left eye sensitivities, the contralateral eye is not blind to the stimulus.

### ERGs

ERGs were recorded at P60 for the rats, or 42 days after transplantation, using an SEIM Biomedical system. For the transplantation experiments, test eyes received superior subretinal injections of 50,000 transduced RPE cells. A double-blind protocol was employed such that the person performing the ERGs did not know which eye received transplantation, which eye remained untreated, and which eye received RPE-GFP and RPE-OTX2. Following overnight dark adaptation, animals were prepared for recording under dim red light. Animals were anaesthetized with intraperitoneal injection of ketamine (100 mg/kg) and xylazine (10 mg/kg) and kept warm with a thermostatically controlled heat platform at 37°C. The pupils were dilated using 0.5% mydriaticum, and the cornea was locally anesthetized with application of chlorhydrate of oxybuprocaine 1.6 mg in 0.4 mL. Upper and lower lids were retracted to keep the eye open and proptosed. Viscotears liquid gel was placed on each cornea to keep it moistened after corneal contact by golden electrodes. A stainless-steel reference electrode was inserted subcutaneously on the head of the rat, and a second needle electrode inserted subcutaneously in the back of the rat grounded the signal. Animals were left for a further 5 min in complete darkness before recording. Ganzfeld ERGs were obtained simultaneously from both eyes to provide an internal control. For scotopic recordings, single flash recordings were obtained at light intensities of 3 μcd $\times$ s/m$^2$, 30 cd $\times$ s/m$^2$, 0.3 cd $\times$ s/m$^2$, and 3 cd $\times$ s/m$^2$ using a sampling frequency of 5 kHz, a flash duration of 4 ms, and a frequency stimulus of 0.5 Hz. Data were recorded from 50 ms before stimulus onset to 450 ms post-stimulus. Photopic cone ERGs were performed on a rod-suppressing background after 5 min of light adaptation; recordings were obtained at light intensities of 10 cd $\times$ s/m$^2$. The band-pass filter was set between 0 and 1 kHz. Each scotopic response represents the average of ten responses and each photopic ERG response represents the average of 5 responses from a set of five flashes of stimulation. The mean time to b-wave peak for each group (n = 7) was determined in each recording. Flicker cone ERG responses were performed with a flashlight at 10 Hz and with intensities of 0.3 cd $\times$ s/m$^2$. Row data are provided in Figures S3–S5.

### OCT

Treated rats at P60 were anesthetized and pupils were dilated as described earlier. Eye dehydration was prevented by regular instillation of sodium chloride drops. OCT images were recorded for both eyes using a spectral domain ophthalmic imaging system (spectral domain OCT) (Bioptigen 840 nm HHP, Bioptigen, North Carolina). Rectangular scans consisting of a 2 by 2 mm perimeter, with 1,000 A scans per B scan and a total B-scan amount of 100, were scored. Scans were obtained first while centered on the optic nerve and then with the nerve either displaced temporally or nasally or displaced superiorly or inferiorly. OCT scans were exported from InVivoVue as audio video interleave (AVI) files. These files were loaded into ImageJ v.1.47 (NIH, Bethesda, MD), where they were registered using the Stackreg plug-in. Scaling of the image was performed converting the number of pixels to a distance of 3.11 pixels/μm. ONL thickness was measured every 100 μm, ventral-dorsal and temporal to nasal, starting from the optic nerve and covering the retinal area given by OCT scan using a homemade plugin for ImageJ. The mean of the thickness of each point was calculated for the groups untreated eye (n = 6), RPE-GFP transplanted eye (n = 6), and RPE-OTX2 (n = 7). ONL thickness was represented as 3D density maps.

### In Vivo SLO

High-resolution infrared reflectance imaging and fluorescein angiography were performed with a modified scanning laser ophthalmoscope (SLO) (Heidelberg Retina Angiograph, Heidelberg Engineering, Germany) as previously described.[65,66]

### Live and Dead Assay

Live and dead assay was performed as previously described by Léveillard et al.[7] Briefly, RPE cells transduced with GFP, OTX2, and OTX2L were incubated for 1 week with CDM. Conditioned medium from RPE-transduced cells was collected and was added to primary retina cultures from chicken embryos (stage 29), prepared as described earlier,[67] in 96-well black tissue-culture plates (Corning) and incubated for 7 days at 37°C in 5% $CO_2$. 14 negative control wells (conditioned medium) were also included. We used a live and dead assay (Molecular Probes) to monitor cell viability. A blind protocol was employed such that the person performing the live and dead analysis did not know which supernatant came from RPE-GFP- or RPE-OTX2-transduced cells. For acquisition and cell counting, we developed an algorithm based on the Metamorph software (Universal Imaging). We read plates under an inverted fluorescence microscope (TE 200, Nikon) equipped with a mercury epifluorescent lamp with two excitation filters (485 and 520 nm), two emission filters (520 and 635 nm), a 10× objective, a computer-driven motorized scanning stage (Märzhäuser), and a CCD camera. For the assay, we compared numbers of live cells with the mean number of live cells in the negative controls. Each assay was repeated three independent times with four replicates for each condition.

### Embedding and Toluidine Blue Staining

Animals were anesthetized with ketamine and xylazine as previously described and immediately perfused with 2.5% glutaraldehyde and 2% formaldehyde in PBS. Eyes were enucleated and incubated in fixative (2% formaldehyde) overnight. Lenses were removed, and eyecups were washed 5 times in 5% sucrose. Eyecups were fixed for 1 hr in 2% osmium tetroxide (Sigma-Aldrich 201030). This step was followed by dehydration with graded ethanol (50%, 70%, and 95%) and 10 min of incubation in propylene oxide. Afterward, eyes were incubated overnight at RT with a 1:1 mixture of araldite-epoxy resin and propylene oxide. Embedding was done with araldite-epoxy resin mixture warmed at 65°C overnight. Plastic sections of 1 μm thickness were made along the sagittal axis using Leica EM UC6 ultramicrotome and stained with toluidine blue (1% Borax, 1% toluidine blue).

### Statistics

All data are expressed as means ± SE, unless otherwise stated. n = number of animals, eyes, or cells examined, as appropriate. Statistical significance was assessed using GraphPad Prism 6 software and applying unpaired non-parametric t test, ANOVA with Bonferroni or Dunnett's correction for multiple comparisons, Welch correction, Kolmogorov-Smirnov, and Wilcoxon matched pairs (two-tailed), where appropriate.

## SUPPLEMENTAL INFORMATION

Supplemental Information includes six figures and one table and can be found with this article online at https://doi.org/10.1016/j.ymthe.2017.09.007.

## AUTHOR CONTRIBUTIONS

C.K.: Figures 1A, 1C–1E, 2A–2C, 2E, 3A–3D, 4A–4G, 5A–5D, 6A–6I, 7A–7D, 8F, S1–5, and S6A and writing the manuscript. L.K.: Figures 4A–4I, 6A–6I, and 8G. YY: Figures 4A–4G, 5A–5D, 6A–6I, S6B, and S6C and writing the manuscript. V.F.: Figures 7A–7D. F.B.: Figures 1C, 2E, 2F, and 6B. S.R.: Figures 1B, 2D, 3A, 3B, and S1. G.M.-P.: Figures 1B, 2D, 8A, 8B, and 8E. E.C.: Figure 8D. N.A.-A.: Figure 8F. D.P.: Figures 4H and 4I. H.C.: Figure 1E. M.D.: Figure 1E. E.F.N.: Figures 4H and 4I. J.S.: scientific advices transplantation. O.G.: scientific advices and biological material iPSCs. T.L.: principal investigator and writing the manuscript.

## ACKNOWLEDGMENTS

We thank A. Bemelmans for providing biological material. We thank D. Zack, J. Bennicelli, and J. Bennett for technical and scientific help. This work was supported by INSERM, Université Pierre and Marie Curie, and Fondation Voir & Entendre.

## REFERENCES

1. Ryan, S.J. (2006). Retina (Elsevier Mosby).

2. Ksantini, M., Lafont, E., Bocquet, B., Meunier, I., and Hamel, C.P. (2012). Homozygous mutation in MERTK causes severe autosomal recessive retinitis pigmentosa. Eur. J. Ophthalmol. *22*, 647–653.

3. Bowne, S.J., Humphries, M.M., Sullivan, L.S., Kenna, P.F., Tam, L.C., Kiang, A.S., Campbell, M., Weinstock, G.M., Koboldt, D.C., Ding, L., et al. (2011). A dominant mutation in RPE65 identified by whole-exome sequencing causes retinitis pigmentosa with choroidal involvement. Eur. J. Hum. Genet. *19*, 1074–1081.

4. Gal, A., Li, Y., Thompson, D.A., Weir, J., Orth, U., Jacobson, S.G., Apfelstedt-Sylla, E., and Vollrath, D. (2000). Mutations in MERTK, the human orthologue of the RCS rat retinal dystrophy gene, cause retinitis pigmentosa. Nat. Genet. *26*, 270–271.
5. Zhang, W., Zhang, X., Wang, H., Sharma, A.K., Edwards, A.O., and Hughes, B.A. (2013). Characterization of the R162W Kir7.1 mutation associated with snowflake vitreoretinopathy. Am. J. Physiol. Cell Physiol. *304*, C440–C449.
6. Bennett, J., Ashtari, M., Wellman, J., Marshall, K.A., Cyckowski, L.L., Chung, D.C., McCague, S., Pierce, E.A., Chen, Y., Bennicelli, J.L., et al. (2012). AAV2 gene therapy readministration in three adults with congenital blindness. Sci. Transl. Med. *4*, 120ra15.
7. Léveillard, T., Mohand-Saïd, S., Lorentz, O., Hicks, D., Fintz, A.C., Clérin, E., Simonutti, M., Forster, V., Cavusoglu, N., Chalmel, F., et al. (2004). Identification and characterization of rod-derived cone viability factor. Nat. Genet. *36*, 755–759.
8. Byrne, L.C., Dalkara, D., Luna, G., Fisher, S.K., Clérin, E., Sahel, J.A., Léveillard, T., and Flannery, J.G. (2015). Viral-mediated RdCVF and RdCVFL expression protects cone and rod photoreceptors in retinal degeneration. J. Clin. Invest. *125*, 105–116.
9. Yang, Y., Mohand-Said, S., Danan, A., Simonutti, M., Fontaine, V., Clerin, E., Picaud, S., Léveillard, T., and Sahel, J.A. (2009). Functional cone rescue by RdCVF protein in a dominant model of retinitis pigmentosa. Mol Ther. *17*, 787–795.
10. Girman, S.V., Wang, S., and Lund, R.D. (2005). Time course of deterioration of rod and cone function in RCS rat and the effects of subretinal cell grafting: a light- and dark-adaptation study. Vision Res. *45*, 343–354.
11. Algvere, P., Berglin, L., Gouras, P., and Sheng, Y. (1994). Transplantation of fetal retinal pigment epithelium in age-related macular degeneration with subfoveal neovascularization. Graefes Arch. Clin. Exp. Ophthalmol. *232*, 707–716.
12. Coffey, P.J., Girman, S., Wang, S.M., Hetherington, L., Keegan, D.J., Adamson, P., Greenwood, J., and Lund, R.D. (2002). Long-term preservation of cortically dependent visual function in RCS rats by transplantation. Nat. Neurosci. *5*, 53–56.
13. Binder, S., Stolba, U., Krebs, I., Kellner, L., Jahn, C., Feichtinger, H., Povelka, M., Frohner, U., Kruger, A., Hilgers, R.D., and Krugluger, W. (2002). Transplantation of autologous retinal pigment epithelium in eyes with foveal neovascularization resulting from age-related macular degeneration: a pilot study. Am. J. Ophthalmol. *133*, 215–225.
14. da Cruz, L., Chen, F.K., Ahmado, A., Greenwood, J., and Coffey, P. (2007). RPE transplantation and its role in retinal disease. Prog. Retin. Eye Res. *26*, 598–635.
15. Del Priore, L.V., Kaplan, H.J., Tezel, T.H., Hayashi, N., Berger, A.S., and Green, W.R. (2001). Retinal pigment epithelial cell transplantation after subfoveal membranectomy in age-related macular degeneration: clinicopathologic correlation. Am. J. Ophthalmol. *131*, 472–480.
16. Salero, E., Blenkinsop, T.A., Corneo, B., Harris, A., Rabin, D., Stern, J.H., and Temple, S. (2012). Adult human RPE can be activated into a multipotent stem cell that produces mesenchymal derivatives. Cell Stem Cell *10*, 88–95.
17. Casaroli-Marano, R.P., Pagan, R., and Vilaró, S. (1999). Epithelial-mesenchymal transition in proliferative vitreoretinopathy: intermediate filament protein expression in retinal pigment epithelial cells. Invest. Ophthalmol. Vis. Sci. *40*, 2062–2072.
18. Martínez-Morales, J.R., Dolez, V., Rodrigo, I., Zaccarini, R., Leconte, L., Bovolenta, P., and Saule, S. (2003). OTX2 activates the molecular network underlying retina pigment epithelium differentiation. J. Biol. Chem. *278*, 21721–21731.
19. Martínez-Morales, J.R., Rodrigo, I., and Bovolenta, P. (2004). Eye development: a view from the retina pigmented epithelium. BioEssays *26*, 766–777.
20. Tamiya, S., Liu, L., and Kaplan, H.J. (2010). Epithelial-mesenchymal transition and proliferation of retinal pigment epithelial cells initiated upon loss of cell-cell contact. Invest. Ophthalmol. Vis. Sci. *51*, 2755–2763.
21. Booij, J.C., ten Brink, J.B., Swagemakers, S.M., Verkerk, A.J., Essing, A.H., van der Spek, P.J., and Bergen, A.A. (2010). A new strategy to identify and annotate human RPE-specific gene expression. PLoS ONE *5*, e9341.
22. Masuda, T., and Esumi, N. (2010). SOX9, through interaction with microphthalmia-associated transcription factor (MITF) and OTX2, regulates BEST1 expression in the retinal pigment epithelium. J. Biol. Chem. *285*, 26933–26944.
23. Nandrot, E.F., Anand, M., Sircar, M., and Finnemann, S.C. (2006). Novel role for alphavbeta5-integrin in retinal adhesion and its diurnal peak. Am. J. Physiol. Cell Physiol. *290*, C1256–C1262.
24. Nandrot, E., Dufour, E.M., Provost, A.C., Péquignot, M.O., Bonnel, S., Gogat, K., Marchant, D., Rouillac, C., Sépulchre de Condé, B., Bihoreau, M.T., et al. (2000). Homozygous deletion in the coding sequence of the c-mer gene in RCS rats unravels general mechanisms of physiological cell adhesion and apoptosis. Neurobiol. Dis. *7* (6 Pt B), 586–599.
25. Nandrot, E.F., Silva, K.E., Scelfo, C., and Finnemann, S.C. (2012). Retinal pigment epithelial cells use a MerTK-dependent mechanism to limit the phagocytic particle binding activity of αvβ5 integrin. Biol. Cell *104*, 326–341.
26. Nishida, A., Furukawa, A., Koike, C., Tano, Y., Aizawa, S., Matsuo, I., and Furukawa, T. (2003). Otx2 homeobox gene controls retinal photoreceptor cell fate and pineal gland development. Nat. Neurosci. *6*, 1255–1263.
27. Courtois, V., Chatelain, G., Han, Z.Y., Le Novère, N., Brun, G., and Lamonerie, T. (2003). New Otx2 mRNA isoforms expressed in the mouse brain. J. Neurochem. *84*, 840–853.
28. Hejtmancik, J.F., Jiao, X., Li, A., Sergeev, Y.V., Ding, X., Sharma, A.K., Chan, C.C., Medina, I., and Edwards, A.O. (2008). Mutations in KCNJ13 cause autosomal-dominant snowflake vitreoretinal degeneration. Am. J. Hum. Genet. *82*, 174–180.
29. Sergouniotis, P.I., Davidson, A.E., Mackay, D.S., Li, Z., Yang, X., Plagnol, V., Moore, A.T., and Webster, A.R. (2011). Recessive mutations in KCNJ13, encoding an inwardly rectifying potassium channel subunit, cause leber congenital amaurosis. Am J Hum Genet. *89*, 183–190.
30. Pattnaik, B.R., Shahi, P.K., Marino, M.J., Liu, X., York, N., Brar, S., Chiang, J., Pillers, D.A., and Traboulsi, E.I. (2015). A novel KCNJ13 nonsense mutation and loss of Kir7.1 channel function causes Leber congenital amaurosis (LCA16). Hum Mutat. *36*, 720–727.
31. Reichman, S., Terray, A., Slembrouck, A., Nanteau, C., Orieux, G., Habeler, W., Nandrot, E.F., Sahel, J.A., Monville, C., and Goureau, O. (2014). From confluent human iPS cells to self-forming neural retina and retinal pigmented epithelium. Proc. Natl. Acad. Sci. USA *111*, 8518–8523.
32. D'Cruz, P.M., Yasumura, D., Weir, J., Matthes, M.T., Abderrahim, H., LaVail, M.M., and Vollrath, D. (2000). Mutation of the receptor tyrosine kinase gene Mertk in the retinal dystrophic RCS rat. Hum. Mol. Genet. *9*, 645–651.
33. Pinilla, I., Lund, R.D., and Sauvé, Y. (2004). Contribution of rod and cone pathways to the dark-adapted electroretinogram (ERG) b-wave following retinal degeneration in RCS rats. Vision Res. *44*, 2467–2474.
34. Pinilla, I., Cuenca, N., Sauvé, Y., Wang, S., and Lund, R.D. (2007). Preservation of outer retina and its synaptic connectivity following subretinal injections of human RPE cells in the Royal College of Surgeons rat. Exp. Eye Res. *85*, 381–392.
35. Aït-Ali, N., Fridlich, R., Millet-Puel, G., Clérin, E., Delalande, F., Jaillard, C., Blond, F., Perrocheau, L., Reichman, S., Byrne, L.C., et al. (2015). Rod-derived cone viability factor promotes cone survival by stimulating aerobic glycolysis. Cell *161*, 817–832.
36. Alexander, J.J., Umino, Y., Everhart, D., Chang, B., Min, S.H., Li, Q., Timmers, A.M., Hawes, N.L., Pang, J.J., Barlow, R.B., and Hauswirth, W.W. (2007). Restoration of cone vision in a mouse model of achromatopsia. Nat. Med. *13*, 685–687.
37. Yang, Y., Mohand-Said, S., Léveillard, T., Fontaine, V., Simonutti, M., and Sahel, J.A. (2010). Transplantation of photoreceptor and total neural retina preserves cone function in P23H rhodopsin transgenic rat. PLoS ONE *5*, e13469.
38. Léveillard, T., and Sahel, J.A. (2010). Rod-derived cone viability factor for treating blinding diseases: from clinic to redox signaling. Sci. Transl. Med. *2*, 26ps16.
39. Jacobs, G.H., Fenwick, J.A., and Williams, G.A. (2001). Cone-based vision of rats for ultraviolet and visible lights. J. Exp. Biol. *204*, 2439–2446.
40. Li, Y., Tao, W., Luo, L., Huang, D., Kauper, K., Stabila, P., Lavail, M.M., Laties, A.M., and Wen, R. (2010). CNTF induces regeneration of cone outer segments in a rat model of retinal degeneration. PLoS ONE *5*, e9495.
41. Ayton, L.N., Apollo, N.V., Varsamidis, M., Dimitrov, P.N., Guymer, R.H., and Luu, C.D. (2014). Assessing residual visual function in severe vision loss. Invest. Ophthalmol. Vis. Sci. *55*, 1332–1338.
42. Béby, F., Housset, M., Fossat, N., Le Greneur, C., Flamant, F., Godement, P., and Lamonerie, T. (2010). Otx2 gene deletion in adult mouse retina induces rapid RPE dystrophy and slow photoreceptor degeneration. PLoS ONE *5*, e11673.

43. Housset, M., Samuel, A., Ettaiche, M., Bemelmans, A., Béby, F., Billon, N., and Lamonerie, T. (2013). Loss of Otx2 in the adult retina disrupts retinal pigment epithelium function, causing photoreceptor degeneration. J. Neurosci. *33*, 9890–9904.

44. Karali, M., and Banfi, S. (2015). Inherited retinal dystrophies: the role of gene expression regulators. Int. J. Biochem. Cell Biol. *61*, 115–119.

45. Esumi, N., Kachi, S., Hackler, L., Jr., Masuda, T., Yang, Z., Campochiaro, P.A., and Zack, D.J. (2009). BEST1 expression in the retinal pigment epithelium is modulated by OTX family members. Hum. Mol. Genet. *18*, 128–141.

46. Kusaka, S., Inanobe, A., Fujita, A., Makino, Y., Tanemoto, M., Matsushita, K., Tano, Y., and Kurachi, Y. (2001). Functional Kir7.1 channels localized at the root of apical processes in rat retinal pigment epithelium. J. Physiol. *531*, 27–36.

47. Yang, D., Pan, A., Swaminathan, A., Kumar, G., and Hughes, B.A. (2003). Expression and localization of the inwardly rectifying potassium channel Kir7.1 in native bovine retinal pigment epithelium. Invest. Ophthalmol. Vis. Sci. *44*, 3178–3185.

48. Daniele, L.L., Sauer, B., Gallagher, S.M., Pugh, E.N., Jr., and Philp, N.J. (2008). Altered visual function in monocarboxylate transporter 3 (Slc16a8) knockout mice. Am. J. Physiol. Cell Physiol. *295*, C451–C457.

49. Fritsche, L.G., Chen, W., Schu, M., Yaspan, B.L., Yu, Y., Thorleifsson, G., Zack, D.J., Arakawa, S., Cipriani, V., Ripke, S., et al.; AMD Gene Consortium (2013). Seven new loci associated with age-related macular degeneration. Nat. Genet. *45*, 433–439, e1–e2.

50. Wen, R., Tao, W., Luo, L., Huang, D., Kauper, K., Stabila, P., LaVail, M.M., Laties, A.M., and Li, Y. (2012). Regeneration of cone outer segments induced by CNTF. Adv Exp Med Biol. *723*, 93–99.

51. Schlichtenbrede, F.C., MacNeil, A., Bainbridge, J.W., Tschernutter, M., Thrasher, A.J., Smith, A.J., and Ali, R.R. (2003). Intraocular gene delivery of ciliary neurotrophic factor results in significant loss of retinal function in normal mice and in the Prph2Rd2/Rd2 model of retinal degeneration. Gene Ther. *10*, 523–527.

52. Prochiantz, A., Fuchs, J., and Di Nardo, A.A. (2014). Postnatal signalling with homeoprotein transcription factors. Philos Trans R Soc Lond B Biol Sci. *369*, 20130518.

53. Binder, S., Krebs, I., Hilgers, R.D., Abri, A., Stolba, U., Assadoulina, A., Kellner, L., Stanzel, B.V., Jahn, C., and Feichtinger, H. (2004). Outcome of transplantation of autologous retinal pigment epithelium in age-related macular degeneration: a prospective trial. Invest. Ophthalmol. Vis. Sci. *45*, 4151–4160.

54. Falkner-Radler, C.I., Krebs, I., Glittenberg, C., Povazay, B., Drexler, W., Graf, A., and Binder, S. (2011). Human retinal pigment epithelium (RPE) transplantation: outcome after autologous RPE-choroid sheet and RPE cell-suspension in a randomised clinical study. Br. J. Ophthalmol. *95*, 370–375.

55. Saigo, Y., Abe, T., Hojo, M., Tomita, H., Sugano, E., and Tamai, M. (2004). Transplantation of transduced retinal pigment epithelium in rats. Invest. Ophthalmol. Vis. Sci. *45*, 1996–2004.

56. Lund, R.D., Adamson, P., Sauvé, Y., Keegan, D.J., Girman, S.V., Wang, S., Winton, H., Kanuga, N., Kwan, A.S., Beauchène, L., et al. (2001). Subretinal transplantation of genetically modified human cell lines attenuates loss of visual function in dystrophic rats. Proc. Natl. Acad. Sci. USA *98*, 9942–9947.

57. Delyfer, M.N., Aït-Ali, N., Camara, H., Clérin, E., Korobelnik, J.F., Sahel, J.A., and Léveillard, T. (2013). Transcriptomic analysis of human retinal surgical specimens using jouRNAI. J. Vis. Exp. *78*, e50375.

58. Dalkara, D., Kolstad, K.D., Caporale, N., Visel, M., Klimczak, R.R., Schaffer, D.V., and Flannery, J.G. (2009). Inner limiting membrane barriers to AAV-mediated retinal transduction from the vitreous. Mol. Ther. *17*, 2096–2102.

59. Reichman, S., and Goureau, O. (2016). Production of retinal cells from confluent human iPS cells. Methods Mol. Biol. *1357*, 339–351.

60. Dorval, K.M., Bobechko, B.P., Fujieda, H., Chen, S., Zack, D.J., and Bremner, R. (2006). CHX10 targets a subset of photoreceptor genes. J. Biol. Chem. *281*, 744–751.

61. Pattenden, S.G., Klose, R., Karaskov, E., and Bremner, R. (2002). Interferon-gamma-induced chromatin remodeling at the CIITA locus is BRG1 dependent. EMBO J. *21*, 1978–1986.

62. Reichman, S., Kalathur, R.K., Lambard, S., Aït-Ali, N., Yang, Y., Lardenois, A., Ripp, R., Poch, O., Zack, D.J., Sahel, J.A., and Léveillard, T. (2010). The homeobox gene CHX10/VSX2 regulates RdCVF promoter activity in the inner retina. Hum. Mol. Genet. *19*, 250–261.

63. Prusky, G.T., Alam, N.M., Beekman, S., and Douglas, R.M. (2004). Rapid quantification of adult and developing mouse spatial vision using a virtual optomotor system. Invest. Ophthalmol. Vis. Sci. *45*, 4611–4616.

64. Pearson, R.A., Barber, A.C., Rizzi, M., Hippert, C., Xue, T., West, E.L., Duran, Y., Smith, A.J., Chuang, J.Z., Azam, S.A., et al. (2012). Restoration of vision after transplantation of photoreceptors. Nature *485*, 99–103.

65. Genevois, O., Paques, M., Simonutti, M., Sercombe, R., Seylaz, J., Gaudric, A., Brouland, J.P., Sahel, J., and Vicaut, E. (2004). Microvascular remodeling after occlusion-recanalization of a branch retinal vein in rats. Invest. Ophthalmol. Vis. Sci. *45*, 594–600.

66. Paques, M., Simonutti, M., Roux, M.J., Picaud, S., Levavasseur, E., Bellman, C., and Sahel, J.A. (2006). High resolution fundus imaging by confocal scanning laser ophthalmoscopy in the mouse. Vision Res. *46*, 1336–1345.

67. Adler, R., and Hatlee, M. (1989). Plasticity and differentiation of embryonic retinal cells after terminal mitosis. Science *243*, 391–393.